Tutor/s

Dr. José Francisco García Martínez
Departament d'Enginyeria Química i Química Analítica

Diego Alejandro Ahumada Forigua
Departament d'Enginyeria Química i Química Analítica

Grau de Química

Treball Final de Grau

Simultaneous multi-optical path cell for resource-efficient water quality analysis using commercial reagents.

Cel·la de camí òptic múltiple simultani per a l'anàlisi de la qualitat de l'aigua eficient en recursos mitjançant reactius comercials.

Mateo Rodríguez Castillo

June 2026

Universitat de Barcelona

B:KC Barcelona Knowledge Campus
Campus d'Excel·lència Internacional

Donar exemple no és la principal manera d'influir en els altres. És l'única.

Albert Schweitzer

Vull expressar el meu agraïment a la Unitat de Tecnologia Mecànica i al Servei de Manteniment d'Infraestructures dels Centres Científics i Tecnològics de la Universitat de Barcelona per la fabricació de la cel·la utilitzada en aquest treball. La seva contribució ha permès incorporar una millora clau a la metodologia desenvolupada i obtenir uns resultats i unes conclusions molt més enriquidores.

A Diego Ahumada, les eines i recursos proporcionats al llarg del projecte, que han estat de gran valor malgrat les poques ocasions en què hem pogut coincidir.

Al meu tutor, Jose Francisco, la confiança i la llibertat que m'ha brindat durant el desenvolupament del treball, així com per haver-me apropat al món de la recerca a través d'un projecte tan estimulant com aquest. Les seves observacions i suggeriments han contribuït enormement a la qualitat final d'aquest treball i la meva formació.

Finalment, a totes aquelles persones que, tant dins com fora de l'àmbit de la ciència, m'han ajudat a entendre el món amb curiositat i una insaciable set de coneixement. Gràcies a elles he après a estimar la ciència, a no deixar mai de fer-me preguntes i a gaudir del procés d'aprendre. Res del que soc, ni del que he fet en aquet treball hagues sigut possible sense elles.

REPORT

IDENTIFICATION AND REFLECTION ON THE SUSTAINABLE DEVELOPMENT GOALS (SDG)

The 2030 Agenda for Sustainable Development is structurally underpinned by five foundational pillars—People, Planet, Prosperity, Peace, and Partnership—which conceptualize sustainability not as an isolated environmental goal, but as an interconnected ecosystem. This final degree thesis inherently aligns with this holistic model by developing a decentralized water-monitoring framework. By optimizing resource efficiency and applying the principles of White Chemistry, the project directly targets the synergy between **Planet**—mitigating chemical waste and preventing aquatic degradation—and **Prosperity**, by lowering economic and infrastructural barriers to environmental control. This approach removes specialized technical bottlenecks, empowering local communities (**People**) to actively engage in independent resource management. Within this integrated paradigm, the project establishes a direct connection with specific Sustainable Development Goals (SDGs), rooted in a balanced evaluation of analytical capability, socioeconomic viability, and environmental responsibility.

Main SDG Alignment: Goal 6 (Clean Water and Sanitation)

The structural core of this final degree thesis is conceptually aligned with SDG 6 (Targets 6.3 and 6.b), which focus on monitoring water quality and strengthening the involvement of local communities in environmental management.

Traditional analytical strategies for monitoring chemical species in water often rely on centralized, high-cost laboratory infrastructure. While highly precise, these standard methodologies present inherent limitations in terms of operational agility, geographical accessibility, and resource demands. The primary objective of this project is to address these challenges by exploring a decentralized monitoring framework. By integrating smartphone sensors with digital image colorimetry to target parameters such as phosphates, the project evaluates an alternative that moves the point of analysis directly to the field.

Therefore, the contribution to SDG 6 does not lie in a specific environmental data output, but in the conceptualization of a tool designed to democratize water screening, reducing the logistical dependencies of traditional tracking.

Secondary SDG Alignment: Goal 12 (Responsible Consumption and Production)

The operational philosophy guiding the design of this methodology is inherently linked to SDG 12 (Targets 12.4 and 12.5) through the conceptual application of White Chemistry principles.

Rather than assessing an analytical method solely through conventional operational metrics, this project is built upon a balanced framework where analytical capability, economic viability, and environmental sustainability are evaluated as equally critical vectors. The methodology is structured to minimize the generation of hazardous chemical waste and optimize reagent consumption compared to conventional desktop spectrophotometry.

By evaluating how everyday consumer electronics can be adapted for environmental screening, the project promotes an optimization model that aligns analytical chemistry objectives with a strict reduction in the ecological and material footprint of laboratory practices.

SDG Interconnections: Health, Innovation, and Ecosystem

Beyond its primary targets, the conceptual framework of this methodology creates a cascading alignment with several other global goals. By addressing water screening at its source, the project inherently intersects with SDG 3 (Good Health and Well-being), recognizing that poor water quality and chemical contamination present a direct, structural threat to human health.

Furthermore, if this decentralized model were scaled up and implemented at an industrial or public level, its adoption would represent a significant technological innovation under SDG 9 (Industry, Innovation, and Infrastructure). By replacing cost-prohibitive, traditional laboratory dependence with accessible digital instrumentation, it fosters local technical autonomy and promotes sustainable, low-cost economic growth (SDG 8: Decent Work and Economic Growth).

Finally, the focus on monitoring parameters like phosphates links the project directly to ecological preservation across SDGs 13 (Climate Action), 14 (Life Below Water), and 15 (Life on Land). Uncontrolled nutrient runoff triggers eutrophication, a critical environmental crisis that destabilizes aquatic ecosystems and terrestrial biodiversity alike. By conceptualizing an agile screening tool to detect these imbalances early, the methodology supports immediate climate adaptation and mitigation strategies, protecting vulnerable habitats from ecological collapse across both marine and terrestrial biomes.

Sustainability, Applicability, and the White Chemistry Paradigm

A comprehensive reflection on this project highlights that its core value rests on the development of a highly resource-efficient and environmentally applicable framework. The entire procedural design has been guided by a multi-criteria perspective that systematically links three fundamental pillars:

This integrated approach shifts the focus from traditional "green chemistry" toward the broader paradigm of White Chemistry. Within this framework, environmental safety, industrial applicability, and analytical rigor are treated as interdependent factors. The project aims to demonstrate that a method can be designed to be intrinsically sustainable without demanding a compromise on its operational viability.

From a socio-economic standpoint, designing a protocol around low-cost, readily available hardware ensures its immediate applicability. By conceptualizing a method that eliminates the need for expensive infrastructure, this work addresses the financial and technical barriers that typically restrict environmental testing to specialized institutions.

Consequently, the project lays the groundwork for a scalable model that could allow local communities, agricultural sectors, and decentralized entities to actively participate in independent water quality tracking, turning the principles of the 2030 Agenda into a practical, structural reality.

CONTENTS

1. SUMMARY

Monitoring phosphate levels in aquatic systems is crucial due to its role in environmental eutrophication and the classification of phosphorus as a critical raw material by the European Union.

This degree thesis presents the design, optimization and successful analytical validation of a new simultaneous multiple optical path system integrated with digital image colorimetry (smartphone) that uses commercial reagents for the generation of coloured compounds. The simultaneous multiple optical path cell allows determinations to be made by preparing a single standard of known concentration and with a single dilution of the sample. In this approach, the variation of the concentration is replaced by the variation of the optical path in the application of the Lambert Beer law. The developed configuration allows decentralized, low-cost and sustainable monitoring of phosphate in water resources.

The study included in this work evaluates the capability of commercial procedures for the determination of phosphate concentration, the capability of the use of smartphones as colourimetric detectors and the parameters of the most convenient colour spaces for each determination are determined. The capability for the quantification of the use of different optical paths is also studied. For this application, a cell with multiple simultaneous optical paths is designed and evaluated. The optimized procedure is applied to the determination of different types of water achieving results of quality equivalent to those obtained with spectrophotometric determinations in the laboratory.

The accompanying image (Figure 21) corresponds to the cell with multiple simultaneous optical paths.

Figure 21

Keywords: Water, phosphate, monitoring, colourimetry, smartphone, spectrophotometry, sustainability, analytical chemistry.

2. RESUM

El monitoratge dels nivells de fosfat en els sistemes aquàtics és crucial a causa del seu paper en l'eutrofització ambiental i de la classificació del fòsfor com a matèria primera crítica per part de la Unió Europea.

Aquesta tesi de grau presenta el disseny, l'optimització i la validació analítica exitosa d'un nou sistema de múltiples camins òptics simultanis integrat amb colorimetria d'imatge digital (smartphone) que utilitza reactius comercials per a la generació dels compostos acolorits. La cel.la de múltiples camins òptics simultanis permet realitzar les determinacions mitjançant la preparació d'un únic patró de concentració coneguda i amb una única dilució de la mostra. En aquesta aproximació es substitueix la variació de la concentració per la variació del camí òptic en l'aplicació de la llei de Lambert Beer. La configuració desenvolupada permet el monitoratge descentralitzat, de baix cost i sostenible del fosfat en els recursos hídrics.

L'estudi inclòs en aquest treball avalua la capacitat del procediments comercials per la determinació de la concentració de fosfats, la capacitat de l'ús de smartphones com a detectors colorimètrics i es determinen els paràmetres dels espais de color més convenients per cada determinació. També s'estudia la capacitat per a la quantificació de l'ús de camins òptics diferents. Per aquesta aplicació es dissenya i s'avalua una cel.la de múltiples camins òptics simultanis. El procediment optimitzat s'aplica a la determinació de diferents tipus d'aigües assolint resultats de qualitat equivalent als obtingudes amb les determinacions espectrofotomètriques al laboratori.

La imatge que acompanya (Figura 21) correspon a la cel.la de múltiples camins òptics simultanis.

Figura 21

Paraules clau: Aigua, fosfat, monitoratge, colorimetria, telèfon intel·ligent, espectrofotometria, sostenibilitat, química analítica.

3. INTRODUCTION

3.1. WATER

All biological life is underpinned by water's simple chemical structure. Driven by molecular polarity and hydrogen bonding, its extraordinary capacity as a universal solvent circulates nutrients and sustains global ecosystems. However, this high solubility also makes water resources highly susceptible to contamination. This creates a paradox where the resource required to sustain life frequently becomes a focal point for pollution crises, management challenges, and political conflict.

Although water covers 71% of the Earth's surface, 97.5% of this is saltwater, leaving just 2.5% as freshwater. Much of this freshwater is locked in polar ice and deep aquifers, leaving only 1.2% available as surface water in rivers, lakes and in the atmosphere. Around 70% of this surface water is immobilised in the form of subsoil permafrost. This highly restricted availability means protecting surface water from anthropogenic degradation and reclaiming it is critical for global survival. [1]

Water resources are generally categorised as either natural systems (comprising groundwater and surface waters, such as rivers, lakes and reservoirs) or wastewater (any water degraded by human or animal activity). As untreated wastewater poses severe risks to public health and the environment, rigorous purification and remediation processes are mandatory to neutralise pathogens and restore ecologically viable conditions.

The management of these water resources is governed by specific Royal Decrees (RDs) which regulate quality standards, discharge limits, and criteria for human consumption. Surface water and groundwater standards are set out in RD 817/2015 and RD 35/2023, respectively. The standards for wastewater treatment plant effluents are defined by RD 509/1996 in relation to the anthropogenic cycle, while the criteria for subsequent water reuse are set out in RD 1085/2024. Finally, RD 3/2023 establishes the statutory framework for drinking water quality. Together, these RDs form a comprehensive regulatory framework for pollutant thresholds in all water types. [2, 3, 4, 5, 6]

3.1.1. Phosphorus

Phosphorus is an essential component of biochemistry, found in DNA, RNA, ATP and phospholipids in cell membranes. The thermodynamic instability of its volatile forms means that phosphorus does not exist in significant quantities in the atmosphere. This restricts its biogeochemical cycle to a slow, strictly sedimentary pathway, making phosphorus a limiting nutrient for primary productivity and phytoplankton growth. Undisturbed sedimentation on the ocean floor acts as a terminal sink for phosphorus, trapping it for millions of years and rendering it a finite resource on a human timescale. [7]

In freshwater ecosystems, total phosphorus concentrations exceeding 0.02 mg/L trigger eutrophication, causing massive algal blooms which deplete the amount of dissolved oxygen in the water. The resulting widespread anoxia leads to the mass death of aquatic fauna, critical biodiversity loss, and severe ecosystem degradation. [8]

According to the Stockholm Resilience Centre, global anthropogenic phosphorus discharges amount to 22 million tonnes per year, which is double the safe planetary boundary of 11 million tonnes. This environmental impact is compounded by global supply risks. Morocco holds approximately 70% of global phosphate reserves, creating a geopolitical bottleneck that is further tightened by trade restrictions from major producers such as China. [9, 10]

In order to mitigate geopolitical and environmental strains, the recovery of phosphorus from wastewater can transform the management of resources into a circular paradigm via three main technological processes: struvite precipitation ($MgNH_4PO_4 \cdot 6H_2O$), thermochemical ash leaching, and enhanced biological phosphorus removal (EBPR). [11, 12]

As these circular alternatives are not yet able to offset the regional deficit, the European Union has designated phosphorus as a critical raw material due to total import dependence and a complete absence of biological substitutes. [13]

Phosphorus is introduced into the environment naturally through the geological weathering of apatite minerals. However, human activities, particularly the mining of minerals for use in fertilisers and detergents, significantly accelerate this process. This excess enters aquatic ecosystems via agricultural runoff and municipal wastewater as condensed polyphosphates and organic phosphorus compounds, which subsequently undergo hydrolysis to form the thermodynamically stable orthophosphate ion, PO_4^{3-}. [14]

In environmental matrices, monitoring this chemical transformation requires a clear distinction to be made between the elemental and molecular forms of the chemical. In short, while 1 mg P/L stoichiometrically converts to 3.06 mg PO_4^{3-}/L, this direct ratio is often decoupled in natural or untreated systems due to the presence of unmineralised species such as phospholipids and nucleic acids. [15]

To ensure compliance with environmental and geopolitical imperatives, current legislation sets strict limits for phosphorus species in various water sources. Table 1 outlines these regulatory thresholds and reference guidelines, which cover everything from drinking water standards to the process streams of wastewater treatment plants (WWTPs).

Table 1. Regulatory standards for phosphorus species across water matrices.

Matrix	Parameter	Reference	Range [mg/L]	Notes
Drinking Water	Phosphate (as PO_4^{3-})	RD 3/2023	0.5	Non-mandatory operational value
Surface Water	Total Phosphorus (TP)	RD 817/2015	0.1 – 0.7	To prevent eutrophication
Wastewater (WWTP Influent)	Total Phosphorus (TP)	Typical characterization data	10 – 50	Untreated baseline from domestic/industrial loads
Wastewater (WWTP Effluent)	Total Phosphorus (TP)	RD 509/1996	1.0 – 2.0	Mandatory discharge limit for plants in sensitive areas.

3.2. Colorimetric Analysis

In analytical chemistry, molecular colorimetry quantifies analytes by measuring the attenuation of visible electromagnetic radiation passing through a medium. Many target species, such as orthophosphate, lack intrinsic optical absorption, so the quantitative determination of these requires the controlled synthesis of a stable, intensely coloured chromophore or coordination complex. The Beer–Lambert law governs this optical response, establishing that absorbance, A, is directly proportional to the concentration of the absorbing chemical species, [C], as shown in Equation 1.

$$A = \varepsilon \cdot L \cdot [C]$$

Equation 1. Lambeert-Beer Law

Here, ε is the molar absorptivity coefficient, which is an intrinsic property of the chromophore at a specific wavelength, and L is the optical path length. As both ε and L remain constant under standardised experimental conditions, this law establishes a strict linear correlation that converts macroscopic optical properties into precise, quantitative concentration data. Alternatively, keeping the concentration constant while dynamically modulating the optical path length provides an unconventional but mathematically equivalent dimension for quantitative optical optimization.

3.2.1. Classic Phosphate Quantification

Sophisticated instrumental techniques such as inductively coupled plasma mass spectrometry (ICP-MS) and atomic emission spectroscopy (ICP-AES) offer exceptional sensitivity for determining phosphorus. However, solution-phase colorimetric methods are noteworthy for their operational simplicity and cost-effectiveness in on-site analysis. For water quality monitoring, the two primary chromogenic methods used to quantify phosphates are the molybdenum blue method and the phosphovanadomolybdate method. [16]

The molybdenum blue method is the standard protocol for trace-level analysis, with an operational linearity range of 0.1 mg/L to 1.0 mg/L. Under strongly acidic conditions, orthophosphate reacts with ammonium molybdate to form a 12-molybdophosphoric acid intermediate. The addition of ascorbic acid then selectively reduces the molybdenum atoms within this structure, oxidizing itself to dehydroascorbic acid, described in Equation 2. This electron transfer converts the colourless intermediate into an intense, characteristic blue mixed-valence complex known as molybdenum blue, yielding an absorption maximum in the near-infrared region.

$$PO_4^{3-} + 12\ MoO_4^{2-} + 27\ H^+ \longrightarrow \underset{\text{(colourless)}}{H_3[PMo_{12}^{VI}O_{40}]} + 12\ H_2O \xrightarrow{\text{Ascorbic acid}} \underset{\text{(molybdenum blue)}}{H_3[PMo_{10}^{VI}Mo_2^{V}O_{40}]} + 2\ e^-$$

Equation 2. Two-step reaction pathway for orthophosphate determination via the molybdenum blue method.

For highly concentrated matrices, the molybdate-vanadate method provides a protocol with a wide operational range, spanning from 5 mg/L to 60 mg/L. This mechanism relies on an acid-catalysed direct substitution reaction, in which orthophosphate ions react with ammonium molybdate and ammonium metavanadate. This replaces some of the molybdenum oxides in the framework, synthesising a yellow heteropoly acid complex known as vanadomolybdophosphoric acid, described in Equation 3.

$$PO_4^{3-} + 11\ MoO_4^{2-} + VO_3^- + 25\ H^+ \longrightarrow \underset{\text{(yellow)}}{H_3[PVMo_{11}O_{40}]} + 11\ H_2O$$

Equation 3. One-step reaction pathway for orthophosphate determination via the molybdate-vanadate method.

3.2.2. Commercial Phosphate Quantification

In industrial and environmental monitoring, commercial quantification relies on portable and laboratory photometric systems that are engineered to streamline chromogenic assays deployed in the field. Leading analytical platforms, such as the HANNA Instruments series, use pre-formulated reagents in self-contained digital colorimeters to minimise operational errors outside traditional laboratories.

The low-range HANNA system is designed for trace-level monitoring and has a working range of 0.00 to 2.50 mg/L. This configuration adopts the Standard Methods Ascorbic Acid protocol, in which the targeted chemical reaction between orthophosphate and the commercial reagents produces a characteristic blue colour in the sample. [17]

The high-range HANNA system has been adapted for use with concentrated samples, extending the operational working interval from 0.0 to 30.0 mg/L. This platform uses the amino acid method, in which an amino acid agent initiates a controlled partial redox reaction. By modulating the reduction kinetics, this mechanism effectively moderates the final colour intensity, ensuring that highly concentrated samples remain within a blue absorbance range that can be accurately read by the spectrophotometer. [18]

A comparison of the operating working intervals of the evaluated methods is illustrated in Figure 1.

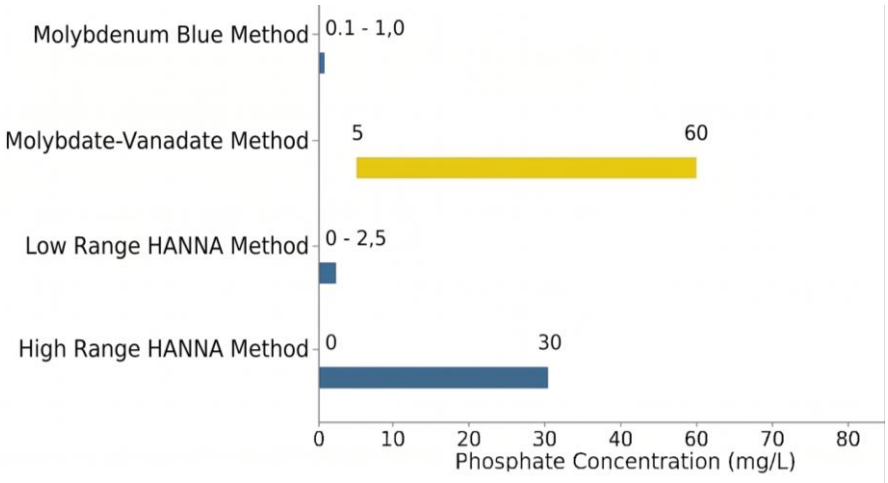

Figure 1. Working intervals for determining phosphates using classical and commercial methods.

The graphical comparison highlights a gap of 1–5 mg/L within traditional methodologies. It should be noted that there is no single standard reference method capable of encompassing this intermediate concentration zone continuously, so alternative or commercial colorimetric systems must be implemented to bridge the gap.

3.2.3. Digital Image Colorimetry

Quantitative Digital Image Colorimetry (DIC) is based on the fundamental principles of the Beer–Lambert law. It uses complementary metal–oxide–semiconductor (CMOS) sensors to convert incident light into digital signals, thereby quantifying the concentration of an analyte. Rather than measuring absorbance at a single wavelength, DIC correlates analyte concentration with changes in colour intensity within the complex's absorption spectrum. [19]

In this framework, the evaluation of colour is based on the extraction of numerical data from standard colour spaces, primarily the additive RGB model. Each pixel is defined by an 8-bit trichromatic vector (R, G, B), yielding integers from 0 to 255 that reflect the sensor's dynamic range. Geometrically, these coordinates define a three-dimensional colour space in which individual pixels are mapped as discrete vector points within a cubic coordinate system, as shown in Figure 2.

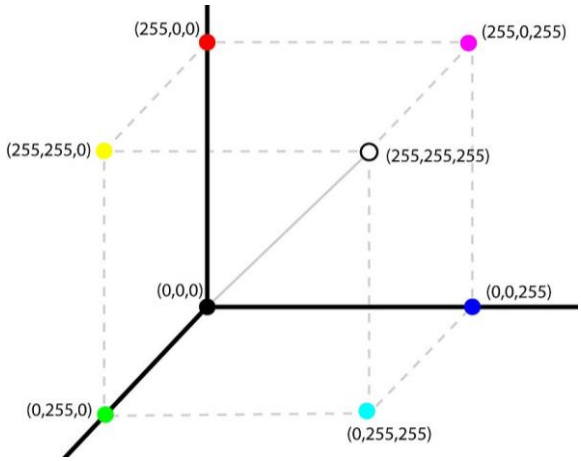

Figure 2. Three-dimensional coordinate system for pixel mapping within the (R, G, B) vector space.

(Ntozis, 7/6/26 via Wikimedia Commons, Creative Commons Attribution)

However, because raw RGB coordinates are highly vulnerable to fluctuations in ambient illumination, analytical robustness requires them to be transformed mathematically into illumination-independent colourimetric parameters, such as brightness, saturation and chromaticity, as summarised in Table 2.

Table 2. Definition and general expressions of RGB-derived colour parameters.

Parameter	General expression	Definition
Brightness	$\frac{R+G+B}{3}$	Average pixel intensity
Saturation	$\frac{\max(R,G,B)-\min(RGB)}{max(R,G,B)}$	Relative purity of a colour; measures the progressive colour shift from a grayscale baseline
Chromaticity_X	$\frac{X}{R+G+B}$	Relative contribution of the X channel to the RGB sum
Ref_X	$\frac{X_{sample}}{X_{blank}}$	Ratio of intensity for channel X between the sample and the blank; used to linearize the instrument response and minimize variations in illumination.

Beyond these fundamental indices, more sophisticated frameworks use matrix and non-linear operations to transform raw RGB data, enhancing calibration robustness against ambient light fluctuations. This approach enables device-dependent data to be converted into perceptually uniform parameters, such as those derived from the CIE *L*u*v** colour space. These parameters include the mean chromatic magnitude, *V_prom_luv*, which functions as a multi-variable expression of the primary channels. [20]

To contextualize the current state of research and assess the scientific impact of smartphone-based colorimetric technologies a bibliometric study was conducted using the SciFinder database. The progressive evolution of scientific publications retrieved under the search query "Smartphone-based Colorimetry" is illustrated in Figure 3-A. To narrow down the focus to the specific scope of this work, the distribution of articles explicitly targeting "Phosphate Smartphone-based Colorimetry" is presented in Figure 3-B.

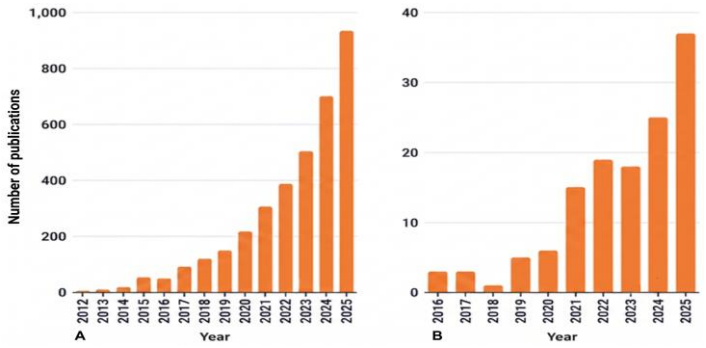

Figure 3. Bibliometric analysis of the literature from the SciFinder database: (A) annual scientific publications under the search query "Smartphone-based Colorimetry" (2012-2025), and (B) subset of articles explicitly targeting "Phosphate Smartphone-based Colorimetry" (2016-2025).

As observed in Figure 3-A, the volume of scientific literature on smartphone-based colorimetry has grown exponentially over the last decade. This upward trend highlights the consolidation of mobile devices as viable analytical tools in modern sensing platforms and the widespread academic interest in them. By contrast, Figure 3-B shows that, although research into phosphate determination via smartphone colorimetry has increased recently, the absolute number of publications remains low. This scarcity highlights that this application is still in its infancy, presenting a significant opportunity for further research and methodological optimisation.

A closer inspection of the most relevant literature in this subset reveals that high-impact studies predominantly focus on the integration of machine learning algorithms to achieve completely equipment-free and versatile quantification across highly diverse water matrices, as well as the implementation of advanced optical designs to drastically elevate sensor sensitivity and enable the simultaneous monitoring of multiple water quality indexes.

3.3. Methodological Sustainability and Applicability Frameworks

To evaluate the viability of newly developed analytical methods, modern chemistry requires a rigorous assessment balancing technical performance, operational applicability, and environmental impact. Green Analytical Chemistry (GAC) utilizes standardized tools like the AGREE metric system—a software-based framework that converts the 12 principles of GAC into a color-coded pictogram based on a mathematical score from 0 to 1—to quantitatively assess sustainability factors such as analysis time, operator requirements, reagent consumption, waste volume, and toxicity. However, this tool exhibits critical limitations, as its algorithm fails to account for crucial socio-economic and operational variables, including labour hour reduction or reagent financial viability. [21] To overcome these limitations, recent paradigms have shifted towards the principles of White Analytical Chemistry (WAC). This holistic framework effectively reconciles environmental safety with both analytical performance and economic-operational viability. This multi-dimensional approach is conceptually structured through a red, blue, and green color-coded balance, illustrated in Figure 4. [22]

Figure 4. White Analytical Chemistry (WAC) framework based on a balanced integration of analytical performance (red), environmental safety (green), and economic-operational viability (blue), resulting in a global white index. *(Reprinted from Nowak et al., 2021; licensed under CC BY 4.0).*

Ultimately, the integration of these frameworks demonstrates that sustainability in modern analytical chemistry is a strictly measurable and quantifiable parameter, rather than a subjective opinion.

4. OBJECTIVES

The primary objective of this thesis is to develop, optimize, and validate a resource-efficient analytical methodology for water quality monitoring, focused on phosphate determination. This is accomplished by combining digital image colorimetry via smartphones with a novel multi-optical path system and commercial reagents, aiming to drastically reduce chemical waste, operational costs, and analysis time without compromising quantitative accuracy.

To this end, the following specific objectives are addressed:

Evaluate spectrophotometric colourimetric methods.

Evaluate smartphone colorimetric determinations at a constant and variable volume.

Develop and model the Simultaneous Multi-Optical Path system (including its application to real water samples).

Evaluate methodological sustainability.

5. EXPERIMENTAL SECTION

5.1. MATERIALS, REAGENTS, AND INSTRUMENTATION

The laboratory apparatus and materials used throughout the experimental phases consisted of volumetric flasks (10, 25, 50 and 100 mL), glass beakers, graduated cylinder (20 mL), a magnetic stirrer, and a hotplate magnetic stirrer. Solutions and sample processing were performed using automatic pipettes ($\pm$ 0.01 mL resolution), an analytical balance ($\pm$ 0.1 mg resolution), Falcon tubes, and plastic syringes equipped with 0,45 μm nylon (NYL) membrane filters. Filter paper and a small glass funnel were employed for gravity filtration steps.

The samples collected for this study are presented and explicitly labelled in Table 3 according to their respective categories and origins. The wastewater matrices consist of the Gavà-Viladecans WWT plant influent, and the treated effluents derived from distinct treatment technologies. The natural waters were drawn from the Ser River and the Consol Spring, all illustrated in Figure 5.

Table 3. Characterization of the selected water samples.

Label	Sample	Category	Origin
M1	WWTP influent	Wastewater	Gavà and Viladecans
M2	WWTP effluent - IFAS treatment	Treated waters	Gavà and Viladecans
M3	WWTP effluent - MBR treatment	Treated waters	Gavà and Viladecans
M4	Ser River	Natural waters	Santa Pau, Girona
M5	Consol Spring	Natural waters	Santa Pau, Girona
M6	Domestic water	Natural waters	Santa Pau, Girona

(a) IFAS treatment removes nutrients by promoting the growth of a specialized biomass. These bacteria are subsequently separated from the water by retaining them on floating plastic carriers.
(b) MBR treatment utilizes the same biological principles as IFAS but relies on membrane ultrafiltration for advanced solid-liquid separation.

Figure 5. Location of the sampled wate resources: Gavà-Viladecans WWTP (left), Ser River (centre), and Consol Spring (right).

All chemical reagents utilized in this study were of analytical or laboratory grade and used as received without additional purification. A certified reference material phosphate standard solution (1000 mg PO_4^{3-}/L, traceable to NIST, Merck) and deionized water were employed to prepare all calibration curves, working standards, and baseline blanks.

For the development of the colorimetric chromogenic complexes, the following reagents were used: ammonium heptamolybdate tetrahydrate, $((NH_4)_6Mo_7O_{24} \cdot 4H_2O$, *pro analysi*, Sigma-Aldrich), L-ascorbic acid ($C_6H_8O_6 \geq 99$ %, Fisher Chemical), ammonium metavanadate ($(NH_4)_6VO_3$, pure, Probus), and potassium sodium tartrate tetrahydrate ($C_4H_4KNaO_6 \cdot 4H_2O$, *puriss*., Sigma-Aldrich).

Acidic reaction environments and matrix digestion conditions were adjusted using sulphuric acid (H_2SO_4, PA-ACS-ISO, 95-98 %, Panreac) and nitric acid (HNO_3, *puriss*., 65 %, Panreac).

Commercial pre-formulated reagent kits were also utilized: Phosphate Low Range kit (HI93713-01, Hanna Instruments), captured in Figure 6-A, utilized via pre-dosed powder packets containing potassium disulfate and potassium antimony tartrate.

Phosphate High Range kit (HI93717-01, Hanna Instruments), consisting of Phosphate HR Reagent A, containing sulphuric acid, and Phosphate HR Reagent B, containing sodium metabisulfite, both shown in Figure 6-B and 6-C, respectively.

Figure 6. Reagents used for commercial phosphate determination: (A) Hanna Instruments LR Reagent powder packet (HI93713-0); (B) Hanna Instruments HR Reagent A liquid dropper bottle (HI93717A-0); and (C) Hanna Instruments HR Reagent B powder packet (HI93717B-0)

Reference UV-Vis absorbance profiles were recorded using an Agilent 8453 G1103A spectrophotometer. Digital colorimetric image acquisition was performed using an Apple iPhone 15 (128 GB, model A1223) as the digital capture device, alongside an 11-inch Apple iPad (128 GB) that served as the transmission light source.

The experimental setup evaluated four distinct types of sample containment devices displayed in Figure 7, consisting of four different geometries and material configurations positioned from left to right. The first device is a standard spectrophotometric cuvette characterized by a fixed 1 cm optical pathlength. Adjacent to it is a multi-well array platform featuring individual containment wells with capacities ranging from a minimum of 0.2 mL to an optimal volume of 1.5 mL, a configuration that ensures a uniform spatial distribution of the liquid phase. The third device is a simultaneous multi-optical path (SMOP) cell fabricated from epoxy resin, structured into 8 independent channels with 8 progressive physical steps each, corresponding to a dilution factor of 10 and step heights of 0.84, 1.26, 1.65, 2.05, 2.46, 2.86, 3.27, and 3.66 cm. The operation of this cell requires a solution volume of 17 mL, approximating as closely as possible the target dilution factor of 10 in the optical pathlength between the shallowest and deepest steps.

The final device is a similar SMOP architecture replicated in polymethyl methacrylate (PMMA), with step heights of 0.85, 1.26, 1.65, 2.04, 2.46, 2.84, 3.26, and 3.67 cm. This acrylic formulation possesses an optically clear, polished, and smooth surface finish that eliminates background fluorescence. The operation of this methacrylate cell requires a solution volume of 18 mL to closely approach the corresponding dilution factor of 10 between its respective pathlengths. All step heights for both CVOP devices were verified using a calliper with a $\pm$0.01 cm precision.

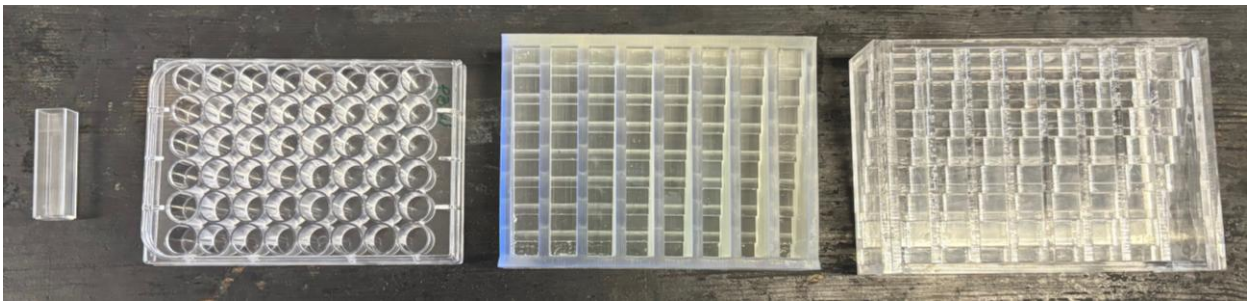

Figure 7. Sample containment devices (from left to right): spectrophotometric cuvette, multi-well plate, epoxy resin SMOP cell, and polymethyl methacrylate (PMMA) SMOP cell.

5.2. METHODS FOR DETERMINING PHOSPHATES

The experimental framework is divided into methods utilizing laboratory reagents and methods utilizing commercial pre-formulated reagents kits. The criterion for the preparation of standard calibration curves consists of covering the known linearity interval of each method, with the specific standards prepared detailed within each corresponding section of the discussion. Additionally, for targeted validation experiments, these concentrations are extended beyond the nominal limits to evaluate and characterize the analytical behaviour and stability limits of the formed chromophore complexes.

5.2.1. Methods for determining phosphates using laboratory reagents

The molybdenum blue composite reagent is prepared on the day of analysis using four independent stock solutions. These solutions consist of a 5 M sulfuric acid solution (6.6 mL of concentrated H_2SO_4diluted carefully to 50 mL with water), an aqueous potassium antimony tartrate solution (0.0686 g diluted to 25 mL), an ammonium molybdate solution (1.00 g to 25 mL, and an L-ascorbic acid solution (0.44 g diluted to 25 mL). To prepare 100 mL of the composite reagent, 50 mL of the prepared sulfuric acid solution, 5 mL of the tartrate solution, 15 mL of the molybdate solution, and 30 mL of the ascorbic acid solution are mixed in this exact sequential order. This final mixture must be used within 4 hours of preparation. For colour development, 8 mL of this composite reagent are added to the sample aliquots or standards inside 50 mL volumetric flasks prior to diluting to the mark with deionized water.

Quantitative measurement is performed via spectrophotometry at a wavelength of 880 nm.

The molybdate-vanadate method involves the direct formation of a yellow heteropoly acid complex. The procedure requires the independent preparation of two stock reagent solutions scaled to 100 mL volumetric flasks: an ammonium vanadate solution, prepared by dissolving 0.25 g in hot deionized water followed by the addition of 2 mL of concentrated HNO_3, and an ammonium molybdate solution, prepared by dissolving 5.0 g in hot water. For colour development, 5 mL of the ammonium molybdate solution, 5 mL of the ammonium vanadate solution, and 1 mL of concentrated HNO_3 are combined inside 50 mL volumetric flasks containing the sample aliquots prior to diluting to the mark with deionized water.

Quantitative determination is performed at an analytical wavelength of 460 nm.

5.2.2. Methods for determining phosphates using commercial reagents

The experimental procedure for the low-range phosphate determination utilizes the commercial HANNA HI93713-01 reagent kit. A clean, dry cuvette is initially filled with 10 mL of the aqueous sample. The entire contents of one packet of HI93713-0 powder reagent are quantitatively added to the solution. The cuvette is subsequently capped and shaken vigorously for approximately 2 minutes to ensure complete dissolution of the solid phase.

Following reagent dissolution, a strict reaction period of exactly 3 minutes is maintained to achieve stable colour development before recording the analytical response at a monitored wavelength of 525 nm.

The quantification of high-range phosphate levels is conducted using the commercial HANNA HI93717 reagent kit. The procedure requires filling a clean, dry cuvette with 10 mL of the sample solution. Sequentially, 10 drops of liquid HR Reagent A (HI93717A-0) and the entire contents of one packet of powder HR Reagent B (HI93717B-0) are introduced into the matrix. The cuvette is capped and gently inverted until the powder is fully dissolved.

The reaction mixture is then allowed to incubate undisturbed for a standardized duration of 5 minutes before the final absorbance measurement is executed at an analytical wavelength of 525 nm.

For commercial runs requiring sample volumes larger than 10 mL (e.g., 20 mL), the operational procedure was uniformly scaled by doubling the added reagent quantities. modification was implemented to maintain a standardized sample-to-reagent ratio, ensuring consistent chemical treatment and analytical reproducibility across all tested matrices without partitioning the original sample volume.

5.3. MEASUREMENT PROCEDURE

5.3.1. Measurement procedure with spectrophotometer

Spectrophotometric measurements were performed to establish an analytical baseline using a conventional benchtop spectrophotometer. For each experimental run, the instrument was initially calibrated by executing a blank measurement using the designated reagent blank in the standard 1 cm cuvette. Following baseline correction, the samples were sequentially introduced into the optical path, ensuring the external walls of the cuvette remained clear and free of artifacts. Absorbance and spectral scans were systematically recorded for each standard and sample solution under identical optical conditions to ensure data reproducibility, configuring the analytical wavelength specifically required for the corresponding method and chromophore complex.

All measurements were carried out under a controlled ambient temperature of approximately 25 °C.

5.3.2. Measurement procedure with smartphone

The instrumental configuration for digital colorimetric measurements comprises a smartphone positioned above an 11-inch tablet, which serves as a regulated backlighting source at a fixed distance of 40 cm. This setup is housed inside a 50 × 50 cm photography box with internal walls lined with matte black and white cardboard to eliminate external illumination interference (Figure 8-A).

Prior to analysis, both devices are powered on for 10 minutes to achieve thermal stabilization. The tablet illumination is set to a fixed intensity between 40% and 50% on a completely horizontal plane, with automatic brightness and power-saving modes deactivated. The smartphone camera is aligned parallel and centred to the illumination matrix using a custom gantry walkway (Figure 8-B), utilizing a fixed 4:3 aspect ratio, a standard exposure baseline, and disabled flash, live photo, and auto-lock features. The measurement sequence is executed via a 5-second shutter timer, consisting of an initial blank background capture, the sample plate capture, and a final background reference capture after plate removal. This standardization mitigates spatial illumination drift, temporal parametric variations, and geometric lens distortions, successfully yielding structured visual matrices for each analysed sample plate, as illustrated in Figure 8-C.

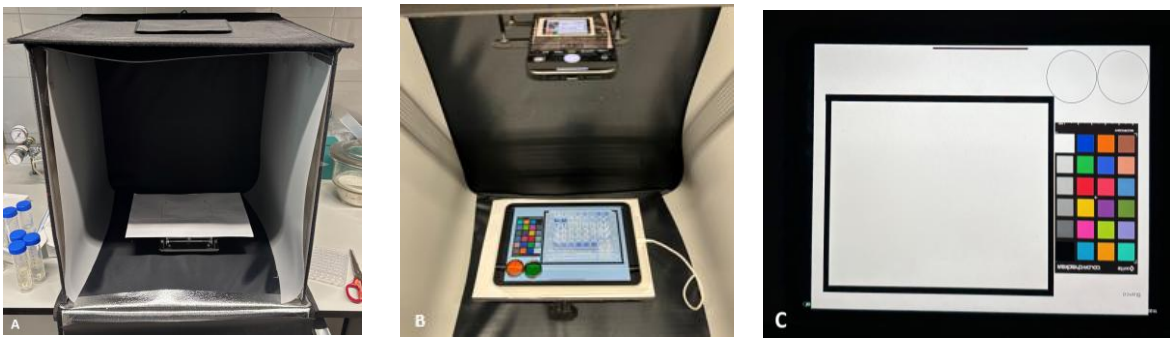

Figure 8. Experimental setup for smartphone-based digital colorimetry: (A) general view of the photography enclosure, (B) internal smartphone and tablet alignment, and (C) captured digital image showing the analysis zone and calibration palette.

5.4. IMAGE ANALYSIS

The image processing and data extraction workflow was executed using a custom RStudio (version 4.5) script architecture developed by D. Ahumada, integrated with ImageJ software.

Initially, the experimental images were exported in .png format to undergo preprocessing. Spatial alignment, smoothing, and precise cropping operations were performed within the RStudio environment utilizing the *imager*, *tcltk*, and *rstudioapi* libraries. This initial step guaranteed geometric uniformity across all sample images prior to numerical extraction.

To mitigate spatial illumination drift caused by the light source, a flat-field correction was subsequently applied to the pre-processed images. This normalization procedure was executed via the *imager* and *tcltk* packages by utilizing a reference photograph of the blank matrix (white tablet background) captured during each individual experiment. A comprehensive comparative analysis evaluating the analytical significance of this tablet blank correction step was detailed in Section 8.X.

Following image rectification, spatial segmentation was executed using ImageJ software to isolate the specific regions of interest corresponding to each sample segment. An automated RStudio script was then deployed to process the segmented regions, calculating mean RGB channel intensities and deriving advanced colorimetric parameters, including multivariate extractions, colour space transformations, and statistical summaries. To establish internal calibration baselines, white, grey, and black reference values were systematically extracted from the standard colour palette positioned adjacent to the sample rack zone within the captured frame, as can be seen in Figure 8-C. These computational procedures, data transformations, and statistical visualizations were executed using a specialized suite of R packages: *png*, *tidyverse*, *magick*, *rgl*, *grid*, *gridExtra*, *ggplot2*, *writexl*, *magrittr*, *reshape2*, *knitr*, *kableExtra*, *ggpubr*, *patchwork*, *colorspace*, *colorscience*, *moments*, *readxl*, *dendextend*, and *EBImage*.

Ultimately, the computational pipeline yielded an exhaustive HTML document compiling the comprehensive image analysis metrics and an XLSX spreadsheet documenting the response of 70 distinct colorimetric parameters across all evaluated segments. This resulting spreadsheet serves as the core data repository for all subsequent statistical treatments.

6. SPECTROPHOTOMETRIC EVALUATION OF COLOURIMETRIC METHODS

6.1. CHARACTERIZATION AND TEMPORAL STABILITY OF PHOSPHATE COMPLEXES

To determine the optimal operational wavelengths, the UV-Vis spectra of the primary phosphate complexes were characterized. The experimental spectrum of the molybdenum blue complex (Figure 9, left) was evaluated alongside the literature profile of the yellow vanadomolybdate complex (Figure 9, right) to map their absorption bands. Subsequently, the commercial kits were analysed by scanning the absorption profiles of the Low Range (Figure 10, left) and High Range (Figure 10, right) complexes to verify their wavelengths of maximum absorbance.

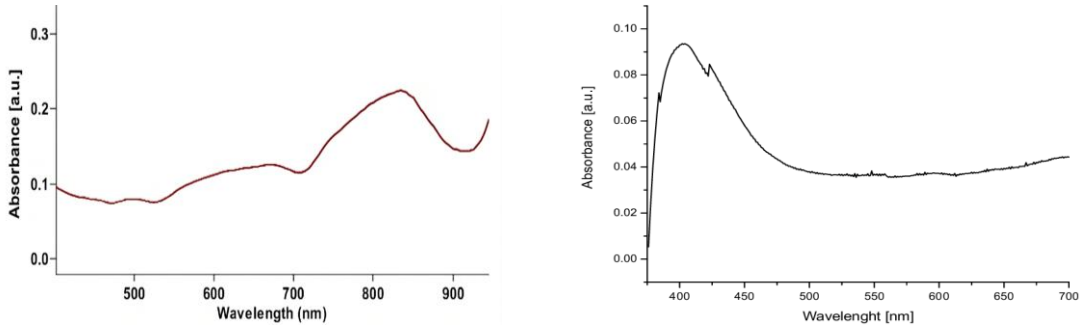

Figure 9. UV-Vis absorption spectra of reference phosphate complexes: (left) experimental spectrum of the molybdenum blue complex, and (right) literature reference spectrum of the yellow vanadomolybdate complex *(adapted from Stadler et al., 2013; licensed under CC BY 4.0).*

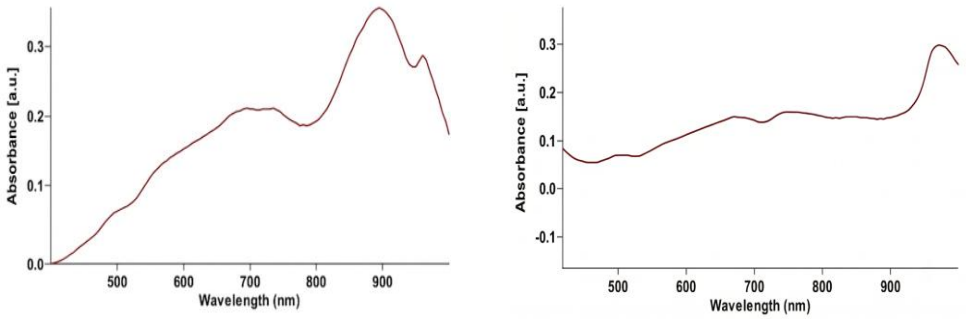

Figure 10. Experimental UV-Vis absorption spectra of complexes obtained using HANNA reagents: (left) Low Range and (right) High Range.

Figure 9 and Figure 10 confirm that the absorbance maxima the blue complexes, both laboratory and commercial, are located near 880 nm. Conversely, the yellow vanadomolybdate complexe exhibit its characteristic spectral bands below 450 nm.

Despite the observed maximum absorbance near 880 nm for the blue complexes, commercial kits operational specifications require measurements at 525 nm. To evaluate the rationale behind this selection, standard phosphate solutions were prepared at 2.0 mg/L for the Low Range (LR) method and 20.0 mg/L for the High Range (HR) method, both within their established working ranges. The absorbance of the resulting complexes was monitored over time at both 880 nm (Figure 11, left) and 525 nm (Figure 11, right) to assess their stability profiles.

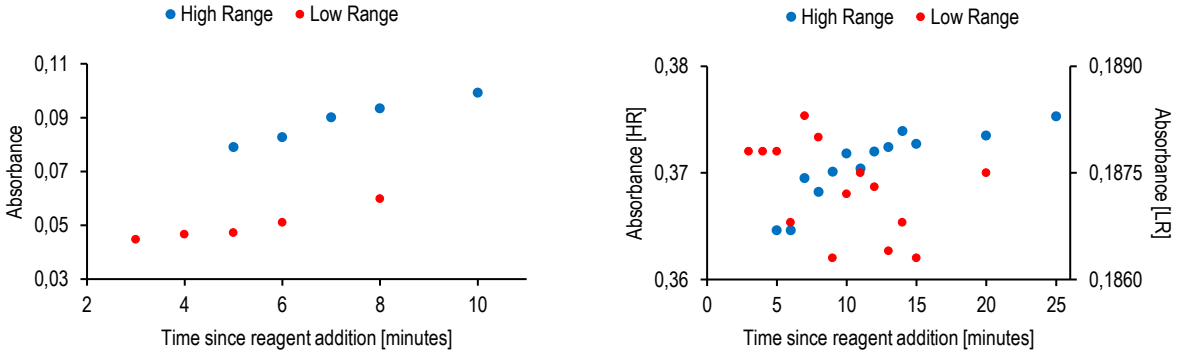

Figure 11. Temporal stability profiles of HANNA commercial reagents monitored at (left) 880 nm and (right) 525 nm for both HR and LR methods.

As shown in Figure 11, measurements at 880 nm reveal a continuous increase in absorbance over time for both methods, whereas at 525 nm, the Low Range method displays no clear trend throughout the monitored period, and the High Range method shows a slight absorbance increase during the first 15 minutes before stabilizing. This enhanced stability at 525 nm aligns with the spectral profiles, as this wavelength sits on a relatively flat region for the blue complexes, minimizing signal fluctuations caused by minor instrumental or chemical variances. Consequently, selecting 525 nm optimizes method robustness over maximum sensitivity, although the precise technical motives behind the manufacturer's choice remain undisclosed.

6.2. QUANTITATIVE PHOSPHATE DETERMINATION USING LABORATORY AND COMMERCIAL REAGENTS

For the quantitative determination of phosphate via external calibration, standard solutions were prepared from 0.10 to 1.00 mg/L for the LR methods and from 5.0 to 60.0 mg/L for the HR methods. These same calibration standards were utilized to test both the laboratory and the commercial reagents, allowing for a direct comparison of their linearity and performance across identical intervals. Figure 12 displays the resulting calibration curves for the LR (left) and HR (right) methods.

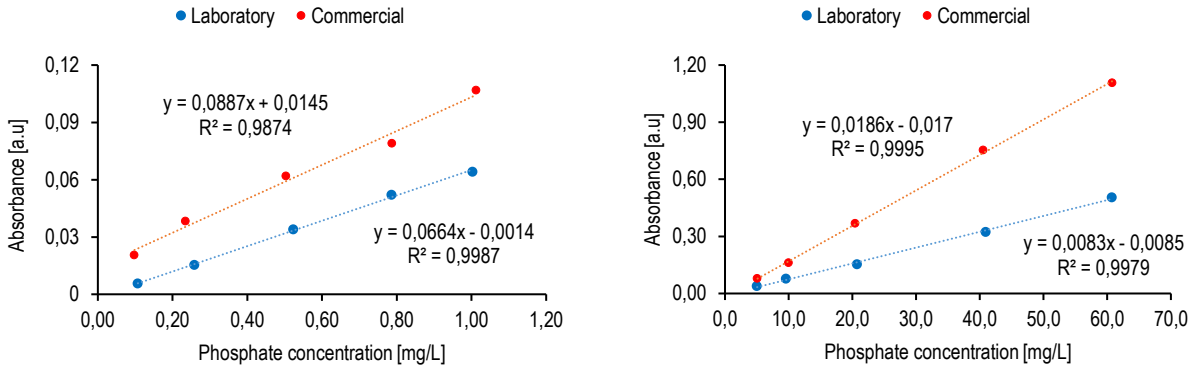

Figure 12. Calibration curves for phosphate determination using laboratory and commercial reagents for (left) LR and (right) HR methods.

Regarding Figure 12 (left), the laboratory LR method demonstrates solid linearity, while the commercial counterpart exhibits a slight deviation. For the HR method (right), both the laboratory and commercial approaches display determination coefficients very close to unity, demonstrating an excellent linearity across the evaluated interval.

To evaluate the analytical performance of each method, five replicates of the same concentration were analysed to determine precision (RSD%), whereas three samples of known concentration were used to assess accuracy (Relative Error %). Based on these data, the figures of merit summarized in Table 4 were obtained, where the Root Mean Square Error (RMSE) was calculated for the calibration phase to offer a more demanding evaluation of the model fit by heavily penalizing outlier points.

Table 4. Validation metrics for the spectrophotometric determination of phosphate across the evaluated methods.

Entry	Method	Interval	Calibration / RMSE [%]	Precision / RSD [%]	Accuracy / RE [%]
1	Molybdenum blue	0.10 mg/L – 1.00 mg/L	2.12	2.74	4.89
2	Molybdate-vanadate	5.0 mg/L – 60.0 mg/L	7.37	1.32	8.08
3	HANNA Low Range	0.10 mg/L – 1.00 mg/L	15.81	4.58	22.55
4	HANNA High Range	5.0 mg/L – 60.0 mg/L	2.32	1.26	0.80

According to Table 4, both laboratory methods and the High Range commercial kit demonstrate solid analytical performance with low error metrics, whereas the Low Range commercial kit exhibits a significant drop in robustness, with its RMSE exceeding 15% and relative error surpassing 20%. These results align with manufacturer specifications as the Low Range kit shows higher deviations at trace levels due to its 0.0 to 2.5 mg/L design, while the High Range kit—originally optimized for 0.0 to 30.0 mg/L—demonstrates excellent linearity and stability even when its application is extended up to 60.0 mg/L, doubling its upper concentration limit without compromising quality. It can be concluded that while commercial reagents are viable for streamlining subsequent work, laboratory-prepared alternatives will continue to be systematically used alongside them for comparative validation.

7. SMARTPHONE EVALUATION FOR COLOURIMETRIC DETERMINATIONS AT A CONSTANT VOLUME

In this section, smartphone-based digital image capture for colourimetric determination was evaluated. For this purpose, standard solutions were analysed via external calibration using a five-point curve and a reagent blank, alongside three samples of known concentration and five replicates of the same concentration. The same analytical methodology described in the previous section was followed. Quantification was performed through, yielding the colour development profiles displayed in Figure 13. Specifically, the image illustrates the captured standards and samples for the laboratory HR approach (left), the commercial HR kit (middle), and both LR methods combined within a single image capture (right).

Figure 13. Smartphone-captured images of the colour development profiles for phosphate quantification: laboratory HR approach (left), commercial HR kit (middle), and both LR methods combined within a single image capture (right).

7.1 SELECTION OF COLOUR SPACE PARAMETERS USING CONSTANT VOLUME

Capability of smartphones and best colour space parameters were assessed at simultaneously. For this purpose, the calibration performance, precision, and accuracy of the 70 image parameters obtained from data processing were systematically evaluated. Based on the correlation between the analytical signal and the standard concentrations, these parameters were ordered to select the three best candidates for final method validation. Additionally, the calibration curve of the top-performing parameter among the three selected is displayed for each method. Table 5 summarizes the analytical performance of the three selected image parameters, while Figure 14 displays the calibration curve of the top-performing candidate for both **laboratory and commercial high-range method.**

Table 5-A. Validation metrics for the determination of phosphate via smartphone colorimetry using the molybdate-vanadate method.

Entry	Parameter	Interval	Calibration / RMSE [%]	Precision / RSD [%]	Accuracy / RE [%]
1	Chromaticity_R	5.0 mg/L – 60.0 mg/L	6.71	6.77	15.18
2	Chromaticity_B	5.0 mg/L – 60.0 mg/L	7.30	7.80	18.71
3	Chromaticity_G	5.0 mg/L – 60.0 mg/L	8.27	8.95	22.35

Table 5-B. Validation metrics for the determination of phosphate via smartphone colorimetry using HANNA HR method.

Entry	Parameter	Interval	Calibration / RMSE [%]	Precision / RSD [%]	Accuracy / RE [%]
1	Chromaticity_R	5.0 mg/L – 60.0 mg/L	4.40	1.67	1.88
2	L_prom_luv	5.0 mg/L – 60.0 mg/L	7,31	1.84	12.16
3	Chromaticity_B	5.0 mg/L – 60.0 mg/L	8.86	0.79	6.86

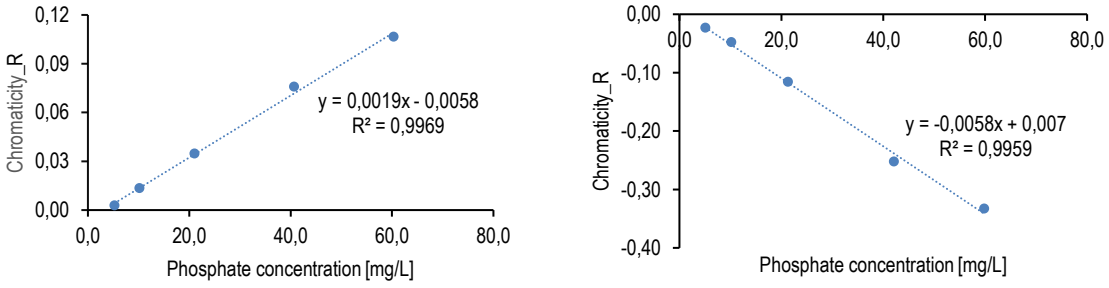

Figure 14. Calibration curves for high-range phosphate determination using the *Chromaticity_R* parameter as the analytical signal: laboratory approach (left) and commercial kit (right).

According to the results summarized in Table 5-A, the laboratory molybdate-vanadate method yields low calibration and precision error metrics with all values remaining below 9% (also showed in Figure 14, left). However, accuracy values exhibit higher deviations, consistently exceeding 15% across all evaluated parameters. Given that this method involves analyzing a yellow-colored complex, the inclusion of *Chromaticity_G* among the top three parameters is chemically coherent; this parameter is highly sensitive to yellow shades, unlike the blue complexes evaluated in the other methods where it does not reappear.

The commercial HANNA HR method (Table 5-B) demonstrates a significantly superior analytical performance, showing overall excellent calibration results and precision errors below 2%. Regarding the selected parameters, the *L_prom_luv* coordinate appears as a top candidate because the high analyte concentrations generate highly darkened blue complexes, making lightness variations a sensitive analytical signal despite its 12% accuracy error.

Table 6 summarizes the analytical performance of the three selected image parameters, while Figure 15 displays the calibration curve of the top-performing candidate for both **laboratory and commercial low-range method.**

Table 6-A. Validation metrics for the determination of phosphate via smartphone colorimetry using molybdenum blue method.

Entry	Parameter	Interval	Calibration / RMSE [%]	Precision / RSD [%]	Accuracy / RE [%]
1	Saturation	0.01 mg/L – 1.00 mg/L	12.91	4.02	8.11
2	Chromaticity_R	0.01 mg/L – 1.00 mg/L	23.76	7.66	8.49
3	Chromaticity_B	0.01 mg/L – 1.00 mg/L	31.25	4.72	10.42

Table 6-B. Validation metrics for the determination of phosphate via smartphone colorimetry using HANNA LR method.

Entry	Parameter	Interval	Calibration / RMSE [%]	Precision / RSD [%]	Accuracy / RE [%]
1	V_prom_luv	0.01 mg/L – 1.00 mg/L	11.45	9.73	12.88
2	Chromaticity_B	0.01 mg/L – 1.00 mg/L	12.45	10.76	10.90
3	Chromaticity_R	0.01 mg/L – 1.00 mg/L	14.82	11.56	11.47

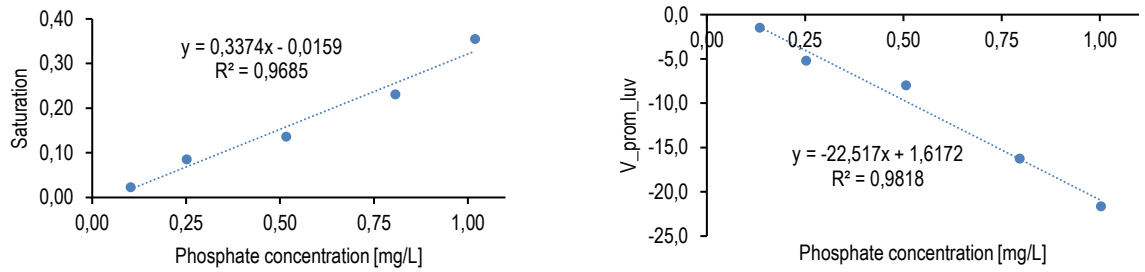

Figure 15. Calibration curves for low-range phosphate determination using the *Chromaticity_R* parameter analytical sign (left) for laboratory approach and *V_prom_luv* (right) for commercial kit.

On the other hand, the laboratory LR method (Table 6-A) presents more acceptable accuracy error metrics, with values remaining below 15%. However, this approach exhibits slightly higher precision errors compared to the commercial alternative under these low concentration conditions.

Table 6-B results demonstrate a significant deviation in the commercial HANNA LR calibration metrics, although precision errors remain relatively low at around 5%. Regarding the selected parameters, the prominence of the *Saturation_S* coordinate emerges as the top candidate because the low analyte concentrations generate highly diluted, faint blue solutions, making saturation variations the most sensitive analytical signal among the otherwise poorly performing parameters.

Figure 15 demonstrates that the calibration curves maintain solid linearity even at the extremes of the operational range using this digital colorimetry approach, contrasting with conventional spectrophotometric measurements that typically deviate at those limits. Conversely, Figure Y does not exhibit this behaviour, although the overall results prove that this digital image methodology has the potential to reach such ideal linearity.

8. SMARTPHONE EVALUATION FOR COLOURIMETRIC DETERMINATIONS AT A VARIABLE VOLUME

In this section, we evaluate the possibility of replacing concentration variation with variation in the optical path to generate signals of different intensities that allow for the calibration process. This study uses laboratory methods, commercial methods, and a smartphone. The experimental procedure was carried out using the same multi-well plate setup from the previous section. For each range, two standard stock solutions of different concentrations were prepared to cover the maximum working range and evaluate whether the linearity interval could be extended for each method. Volumes of the more diluted standard were added to the wells starting from 0.05 mL up to 1.50 mL at 0.1 mL intervals, and the same volumetric scaling was replicated for the concentrated standard. Additionally, a series of reagent blanks was prepared following the exact same volume increments (from 0.05 mL to 1.00 mL) to ensure a rigorous comparison. Volumes below 0.2 mL were discarded from the analysis because they failed to completely cover the well surface, leading to an inhomogeneous solution distribution that would alter the optical measurements. The finalized image captures obtained for each method are displayed in Figure 16.

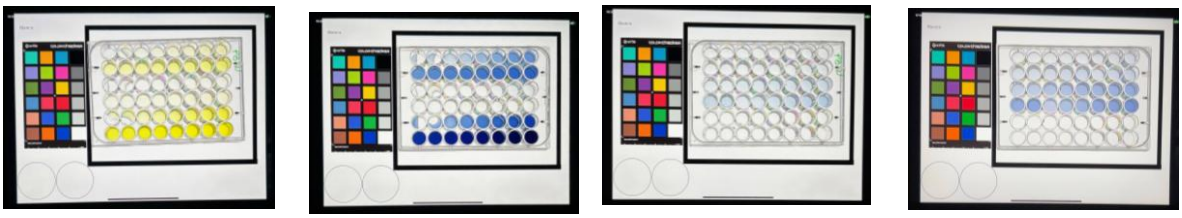

Figure 16. Smartphone-captured images of the volumetric profiling for phosphate quantification. From left to right: laboratory HR (first), commercial HR (second), laboratory LR (third), and commercial LR (fourth).

8.1 SELECTION OF COLOUR SPACE PARAMETERS USING VARIABLE VOLUMES

In this case, the influence of volume and the study of colour space parameters were studied simultaneously. Data processing was standardized by defining an apparent concentration (Equation 4), normalizing all paths to the maximum volume of 1.5 mL. Consequently, this normalization yields an apparent concentration profile that scales proportionally with the dosage volume.

$$C_{apparent} = C_{real} / V_{max}$$

Equation 4. Apparent concentration expression for variable volume system.

Method precision was determined by exploiting the overlapping concentrations obtained from the two different stock solutions across the same volumetric range. Three wells were randomly selected as validation samples to assess accuracy and excluded from the calibration set. The remaining points were used to construct the calibration curves, discarding any outliers. Finally, the linear working range was defined based on the remaining points, and the figures of merit were established.

Following the systematic ranking of the image parameters based on their calibration performance, a consistent pattern emerged across all four methods. Despite minor variations in the ordering, the exact same top-performing parameters were consistently selected. Consequently, *Chromaticity_R*, *Chromaticity_B*, and *V_prom_luv* were established as the optimal parameters and chosen as the definitive analytical signals for all subsequent evaluations. The analytical performance of the three selected image parameters for **commercial phosphate determination** under variable volume conditions is summarized in Table 7-A (HR) and Table 7-B (LR), while the comprehensive validation matrices for the laboratory methodologies are detailed in Appendix 1 (Tables 1.1 and 1.2).

Table 7-A. Validation metrics for digital colorimetry determination evaluating variable volumes for HANNA HR method.

Entry	Parameter	Interval	Calibration / RMSE [%]	Precision / RSD [%]	Accuracy / RE [%]
1	Chromaticity_R	6.5 mg/L – 50.0 mg/L	6.33	5.94	8.02
2	Chromaticity_B	6.5 mg/L – 50.0 mg/L	5.77	3.77	6.10
3	L_prom_luv	6.5 mg/L – 100.0 mg/L	6.66	3.58	3.21

Table 7-B. Validation metrics for digital colorimetry determination evaluating variable volumes for HANNA LR method.

Entry	Parameter	Interval	Calibration / RMSE [%]	Precision / RSD [%]	Accuracy / RE [%]
1	Chromaticity_R	0.40 mg/L – 3.00 mg/L	3.81	1.45	2.91
2	Chromaticity_B	0.40 mg/L – 3.00 mg/L	4.42	1.09	3.20
3	V_prom_luv	0.40 mg/L – 3.00 mg/L	5.36	8.38	5.37

The commercial HR method (Table 7-A) demonstrates a wider linear range that extends down to 6.5 mg/L while keeping consistent analytical performance, as all errors remain below 9%. Notably, instead of the *V_prom_luv* parameter, the *L_prom_luv* coordinate (belonging to the same colour space) emerged as an exceptional signal, exhibiting solid linearity up to 100 mg/L and doubling the operational working interval. According to Table 1.1 (see Appendix 1), the linear working range for the laboratory HR method has been narrowed down to 7.0–50.0 mg/L, as deviations from linearity occur outside these limits. However, by applying this range restriction, all the validation metrics show an improvement compared to the constant volume approach, with no error values exceeding 7%.

Regarding Table 1.2 (see Appendix 1), the lower limit of the working range was raised to 0.40 mg/L due to highly dispersed calibration data below this threshold. However, the upper limit was extended up to 3.00 mg/L, tripling the operational range observed in previous sections. Under these conditions, the calibration errors hover around 10%, but both precision and accuracy metrics show consistent performance. The commercial LR method (Table 7-B) exhibits better overall analytical performance, confirming that the commercial reagents provide an improvement over the laboratory method for low-range determinations using volumes variations.

The increase of the low limit may be a limitation in the analysis of surface water.

8.2. Implementation of an illumination mask for optical positioning standardization

With the aim of improving the analytical results, an illumination mask was implemented over the light source to ensure that the light is directed exclusively to each sample, thereby preventing any individual well from being optically affected by the illumination of adjacent ones. The visual implementation of this stabilization approach across the different tested methods is displayed in Figure 17.

Figure 17. Smartphone-captured images with the illumination mask of the volumetric profiling for phosphate quantification across the studied methods. From left to right: laboratory HR (first), commercial HR (second), laboratory LR (third), and commercial LR (fourth).

The results for the **commercial determination** are summarized in Table 8-A (HR) and Table 8-B (LR), while the comprehensive validation matrices for the laboratory methodologies are detailed in Appendix 2 (Tables 2.1 and 2.2).

Table 8-A. Validation metrics for digital colorimetry at variable volumes using the illumination mask for HANNA HR method.

Entry	Parameter	Interval	Calibration / RMSE [%]	Precision / RSD [%]	Accuracy / RE [%]
1	Chromaticity_R	6.0 mg/L – 60.0 mg/L	7.07	0.83	5.34
2	Chromaticity_B	6.0 mg/L – 60.0 mg/L	6.30	0.29	5.46
3	L_prom_luv	6.0 mg/L – 100.0 mg/L	3.83	0.65	4.84

Table 8-B. Validation metrics for digital colorimetry at variable volumes using the illumination mask for HANNA LR method.

Entry	Parameter	Interval	Calibration / RMSE [%]	Precision / RSD [%]	Accuracy / RE [%]
1	Chromaticity_R	0.40 mg/L – 3.00 mg/L	6.37	0.79	10.12
2	Chromaticity_B	0.40 mg/L – 3.00 mg/L	7.55	0.53	5.08
3	V_prom_luv	0.40 mg/L – 3.00 mg/L	8.77	3.42	6.05

For commercial HR method (Table 8-A), the linear range was expanded, lowering the limit to 6.0 mg/L, and increasing the upper bound to 60.0 mg/L for the chromaticity parameters. While calibration and accuracy do not show significant variations, precision exhibits a clear improvement with the application of the illumination mask. Commercial LR method (Table 8-B) shows that the implementation yields better precision results for the commercial LR approach, although its calibration and accuracy metrics also slightly down. Overall, the results demonstrate that the operational linear range for the low-range methods could not be improved and remains unchanged.

According to Table 2.1 (Appendix 2), the implementation of the illumination mask successfully extends the lower limit of the linear working range down to 5.0 mg/L in laboratory HR method. However, the overall validation metrics remain relatively constant, showing no evident improvement compared to the previous setup. For Table 2.2 (Appendix 2), the laboratory LR method displays a precision enhancement. Accuracy and calibration experience a slight degradation, with the accuracy error worsening by approximately 3%.

In conclusion, although the digital illumination mask accounts for geometric positioning, fails to achieve a precise coverage for every well. This optical stabilization approach does not yield a systematic improvement in calibration and accuracy metrics across the evaluated methods, but it does enhance precision performance. Regarding the operational ranges, the implementation extends the lower limit down to 5.0 mg/L for the HR determinations and extended upper limit of 3.00 mg/L for the LR methods remains stable.

8.3. IMPLEMENTATION OF A BACKGROUND BLANK CORRECTION FOR SIGNAL OPTIMIZATION

With the aim of neutralizing signal drift and correcting illumination inhomogeneities, a pixel-by-pixel background correction was implemented by dividing the sample image by a reference blank image. This mathematical treatment standardizes the light source across the entire multi-well plate, ensuring that all wells are evaluated under identical and stabilized lighting conditions. The visual impact of this background correction is illustrated in Figure 18.

Figure 18. Comparison of the multi-well plate before (left) and after (right) applying the pixel-by-pixel background blank correction.

The resulting analytical parameters after this implementation for the **commercial high-range method** are displayed in Table 9-A, while the comprehensive validation matrices for the remaining three methodologies are detailed in Appendix 3 (Tables 3.1 to 3.3).

Table 9. Comparison of validation metrics for HANNA HR method before and after applying the background blank correction.

Entry	Parameter	Background correction	Calibration / RMSE [%]	Precision / RSD [%]	Accuracy / RE [%]
1	Chromaticity_R	No	6.33	5.94	8.02
2	Chromaticity_R	Yes	4.52	1.68	8.57
3	Chromaticity_B	No	5.77	3.77	6.10
4	Chromaticity_B	Yes	5.19	0.33	6.96
5	L_prom_luv	No	6.66	3.58	3.21
6	L_prom_luv	Yes	3.86	0.28	4.83

The metrics shown in Table 9 suggest this computational treatment leads to a solid improvement in both calibration and precision performance across the board, while accuracy remains stable. The datasets compiled in Appendix 3 show an expansion of the linear range up to 60.0 mg/L and a reduction for the accuracy errors for the laboratory HR approach (Table 1.1). For the commercial LR kit (Table 3.2), the method precision experiences a significant enhancement. In general terms, it can be concluded that the background correction under no circumstances worsens the analytical parameters. Instead, it either maintains equally concordant results or significantly enhances them, proving to be a highly effective and robust technique for digital image colorimetry optimization.

This background blank correction will be systematically applied to all images in the subsequent experimental sections of this work.

9. DEVELOPMENT OF THE SIMULTANEOUS MULTI-OPTICAL PATH METHOD

To minimize the reagents and waste generated during the determination process, and to reduce laboratory time, the use of a cell with simultaneous multiple optical paths (SMOP) built with epoxy resin is proposed. This cell will allow the use of a single standard of known concentration and a single sample dilution. The different optical paths provided by the cell will enable the generation of a sequence of signal intensities using these single solutions. The capability of this approach was assessed by using laboratory and commercial methodologies for LR and HR concentrations levels.

For every methodology, a single standard stock solution was prepared to encompass its entire linear operational range. Three validation samples of known but distinct phosphate concentrations were utilized. To evaluate the method precision, three independent replicates were prepared for the sample concentration and analysed using three separate multi-optical path cells, assessing the reproducibility of the colour parameters. Finally, an additional channel was exclusively allocated to measure the corresponding water blank. The definitive multi-channel image captures obtained through this experimental configuration for each optimized method are displayed in Figure 19.

Figure 19. Smartphone-captured images utilizing the simultaneous multi-optical path cell for phosphate quantification across the studied methods. From left to right: laboratory HR (first), commercial HR (second), laboratory LR (third), and commercial LR (fourth).

9.1. CALIBRATION MODELLING

To establish the analytical calibration model within the simultaneous multi-optical path system, a rigorous sequential data processing protocol was developed. First, the experimental signal acquired from the dedicated blank channel is used to determine the specific background correction for each step of the optical staircase. These blank values are subsequently subtracted from the raw signals of the remaining channels to isolate the net analytical signal contributed exclusively by the analyte, replicating the classic blank correction used in conventional spectrophotometry.

Once the baseline is corrected, the calibration curve is constructed utilizing the data from the standard-containing channels. The apparent concentration for each step of these standard staircases is mathematically modelled by multiplying the nominal concentration of the respective standard solution by its corresponding optical path length factor, b_i, which represents the physical height of each specific step (Equation 5). If the entire cell is designed so that all staircases share identical step heights, this data treatment becomes highly simplified and easily automated.

$$C_{apparent} = C_{real} \cdot b_i$$

Equation 5. Apparent concentration expression for SMOP calibration.

Following the construction of this unified calibration model, the experimental signals from the sample-containing channels are interpolated to determine their respective apparent concentrations. To ensure the mathematical validity of the quantification, an automated filtering criterion is applied: all sample data points falling outside the interpolation limits established by the calibration curve are systematically discarded. To convert these validated apparent concentrations into the real concentration of the sample, this factor is reversed by dividing the apparent values by the specific optical path length of the staircase step where each measurement is located. Theoretically, since each step possesses a known and discrete optical path length, the resulting real concentration calculated across all validated steps for a single sample should converge to an identical, constant value, thereby demonstrating the internal consistency and robustness of the multi-optical path modelling.

This multi-optical path configuration inherently generates a significantly larger dataset per sample compared to conventional single-path spectrophotometry, as a matter of fact, are dilution replicates. From a data processing perspective, this high density of experimental points provides an advantageous tool for extreme cases: it allows for the implementation of stricter filtering criteria to discard potential outliers while still strictly adhering to basic statistical principles, ensuring enough replicates remains to calculate robust accuracy and precision metrics.

9.2. SELECTION OF COLOUR SPACE PARAMETERS FOR SMOP SYSTEM

Given that the precision of the methodologies utilizing variable volumes has previously demonstrated optimal results, the system precision within this framework will be evaluated through the deviation of the entire dataset generated by the calibration algorithm for each specific sample. The validation metrics and parameter selection criteria remain identical to those established in previous sections. Upon evaluating the coordinates that yield the optimal calibration performance, the same parameters and analytical patterns are consistently reproduced. The comprehensive analytical results for this methodology are summarized in Table 10, with each individual.

Table 10-A. Validation metrics for the simultaneous multi-optical path method for molybdate-vanadate determination.

Entry	Parameter	Interval	Calibration / RMSE [%]	Precision / RSD [%]	Accuracy / RE [%]
1	Chromaticity_R	5.0 mg/L – 60.0 mg/L	6.68	18.26	6.27
2	Chromaticity_B	5.0 mg/L – 60.0 mg/L	7.60	6.63	4.22
3	V_prom_luv	5.0 mg/L – 60.0 mg/L	9.72	5.47	1.68

Table 10-B. Validation metrics for the simultaneous multi-optical path method for HANNA HR determination.

Entry	Parameter	Interval	Calibration / RMSE [%]	Precision / RSD [%]	Accuracy / RE [%]
1	Chromaticity_R	5.0 mg/L – 60.0 mg/L	3.01	11.74	14.17
2	Chromaticity_B	5.0 mg/L – 60.0 mg/L	3.93	9.07	2.99
3	V_prom_luv	5.0 mg/L – 60.0 mg/L	4.48	9.09	3.52

Table 10-C. Validation metrics for the simultaneous multi-optical path method for molybdenum blue determination.

Entry	Parameter	Interval	Calibration / RMSE [%]	Precision / RSD [%]	Accuracy / RE [%]
1	Chromaticity_R	0.30 mg/L – 4.00 mg/L	3.04	5.08	0.92
2	Chromaticity_B	0.30 mg/L – 4.00 mg/L	2.30	4.32	1.83
3	V_prom_luv	0.30 mg/L – 4.00 mg/L	3.24	4.01	4.37

Table 10-D. Validation metrics for the simultaneous multi-optical path method for HANNA LR determination.

Entry	Parameter	Interval	Calibration / RMSE [%]	Precision / RSD [%]	Accuracy / RE [%]
1	Chromaticity_R	0.30 mg/L – 6.00 mg/L	6.25	3.32	1.34
2	Chromaticity_B	0.30 mg/L – 6.00 mg/L	6.27	3.86	1.56
3	V_prom_luv	0.30 mg/L – 6.00 mg/L	5.48	3.18	0.76

Regarding the analytical performance for the **high-range determination** summarized in Table 10-A and Table 10-B, several critical aspects must be highlighted. First, the linear working range has been successfully expanded from 5.0 to 60.0 mg/L, matching the limits of conventional spectrophotometers. However, while the precision metrics remain within acceptable limits for most coordinates, the errors associated with accuracy introduce certain limitations. Specifically, for the commercial HR kit (Table 10-B, Entry 1), the *Chromaticity_R* parameter yields a noticeably high accuracy error of 14%, which demands focus the attention to the other colour parameters that provide reasonable results, as similar occurs for the laboratory HR method.

The **low-range determination** (Table 10-C and Table 10-D) demonstrate a robust performance. The linear dynamic range was extended down to 0.30 mg/L for both approaches, reaching an upper limit of 4.00 mg/L for the laboratory method and 6.00 mg/L for the commercial kit. In general terms, none of the calibration, precision, or accuracy errors exceed 7% across the selected colour parameters, confirming that the LR method is fully reliable.

10. APPLICATION TO REAL SAMPLES

To validate the analytical robustness of the simultaneous multi-optical path method under realistic conditions, the system was evaluated using real water samples to assess potential matrix effects that could bias the results. Based on the superior performance demonstrated by the commercial kits in the previous sections, this phase was conducted exclusively utilizing these reagents. To establish a reliable reference and verify the accuracy of the smartphone-based method, the real concentrations of all samples were independently determined using a standard spectrophotometer coupled with the same commercial methods (Table 11).

Table 11. Reference phosphate concentration values for real samples obtained via spectrophotometry using commercial reagents.

Method	M1 [mg/L]	M2 [mg/L]	M3 [mg/L]	M4 [mg/L]	M5 [mg/L]	M6 [mg/L]
Spectrophotometer	24.50	75.53	2.64	0.46	0.54	0.35

10.1. PERFORMANCE EVALUATION OF THE SIMULTANEOUS MULTI-OPTICAL PATH METHOD USING AN EPOXY CELL

For the quantification of the real samples, the same epoxy-based multi-optical path cell described in Section 9 was utilized. To ensure that the sample concentrations would fall within the validated interpolation limits, two external standard solutions were specifically prepared for each determination (HR and LR) to encompass the maximum possible linear range.

Regarding the cell configuration, an independent channel was strictly dedicated to each individual sample blank. This approach effectively compensates for potential matrix effects or background colour interferences unrelated to the phosphate reaction. Due to the physical space required for these sample blanks within the cell architecture, only two distinct real samples could be analysed simultaneously per run. So, the low-range determination (samples M3, M4, M5, and M6) was partitioned and captured across two separate digital photographs. The final digital image captures obtained for these real sample runs are collected in Figure 20.

Figure 20. Smartphone digital image captures for real sample quantification: M1 and M2 (left), M3 and M4 (centre), M5 and M6 (right).

It is worth noting the gradual accumulation of dirt and chemical staining adhered to the cell surface across successive determinations, with the rightmost capture representing the final operational run. This behaviour affects the reuse of cells made with this material.

Following the criteria established in Section 9, the identical colour space parameters were selected to evaluate the quantification of the real water samples. The capacity of the different parameters is evaluated based on the quality of the calibration models obtained in each case. The core analytical parameters are summarized in Table 12. The precision reported in these tables strictly reflects the method precision: it is calculated from the replicates of the different calibration standards that share the same nominal concentration due to being located in equivalent independent staircase steps.

Table 12-A. Validation metrics for SMOP digital colorimetric determination using the HANNA HR method for the analysis of samples M1 and M2.

Entry	Parameter	Interval	Calibration / RMSE [%]	Precision / RSD [%]
1	Chromaticity_R	5.0 mg/L – 50.0 mg/L	3.25	4.41
2	Chromaticity_B	5.0 mg/L – 50.0 mg/L	3.86	2.67
3	V_prom_luv	9.0 mg/L – 90.0 mg/L	3.12	4.04

Table 12-B. Validation metrics for SMOP digital colorimetric determination using the HANNA LR method for the analysis of samples M3 and M4.

Entry	Parameter	Interval	Calibration / RMSE [%]	Precision / RSD [%]
1	Chromaticity_R	0.25 mg/L – 3.5 mg/L	8.79	3.72
2	Chromaticity_B	0.25 mg/L – 3.5 mg/L	5.58	5.69
3	V_prom_luv	0.25 mg/L – 3.5 mg/L	4.89	2.46

Table 12-C. Validation metrics for SMOP digital colorimetric determination using the HANNA LR method for the analysis of samples M5 and M6.

Entry	Parameter	Interval	Calibration / RMSE [%]	Precision / RSD [%]
1	Chromaticity_R	0.25 mg/L – 3.5 mg/L	4.29	1.98
2	Chromaticity_B	0.25 mg/L – 3.5 mg/L	5.15	2.82
3	V_prom_luv	0.25 mg/L – 3.5 mg/L	8.29	3.91

The analytical parameters and calibration performance summarized in Tables 12-A, 12-B, and 12-C consistently align with the trends observed in Section 9. However, certain adjustments in the linear working ranges were identified: for the high-range *Chromaticity_X* parameters, the linearity interval narrowed from 5.0-60.0 mg/L down to 5.0-50.0 mg/L. Conversely, the low-range determinations showed an extension towards lower concentrations, maintaining linearity down to 0.24 mg/L but narrowing its upper limit to 3.5 mg/L. This general reduction in the upper limits of the dynamic ranges could hypothetically be attributed to the gradual accumulation of dirt and chemical staining exhibited by the cell surface, which may slightly degrade the optical response.

Real sample quantification results are distributed as follows: samples M1 and M2 (high-range) are gathered in Table 13-A, while the low-range determinations are split between Table 13-B (samples M3 and M4) and Table 13-C (samples M5 and M6).

Table 13-A. SMOP analytical results for samples M1 and M2 using the HANNA HR method.

Entry	Parameter	M1 [mg/L]	Precision [%]	Accuracy [%]	M2 [mg/L]	Precision [%]	Accuracy [%]
1	Chromaticity_R	25.65	9.57	4.70	71.20	22.94	5.73
2	Chromaticity_B	27.28	2.81	11.35	72.36	13.86	4.20
3	V_prom_luv	24.67	5.33	0.70	80.88	16.60	7.08

Table 13-B. SMOP analytical results for samples M3 and M4 using the HANNA LR method.

Entry	Parameter	M3 [mg/L]	Precision [%]	Accuracy [%]	M4 [mg/L]	Precision [%]	Accuracy [%]
1	Chromaticity_R	2.68	3.00	1.49	0.47	13.49	1.91
2	Chromaticity_B	2.78	3.50	5.27	0.53	5.95	14.92
3	V_prom_luv	2.59	6.39	1.92	0.58	5.19	25.76

Table 13-C. SMOP analytical results for samples M5 and M6 using the HANNA LR method.

Entry	Parameter	M5 [mg/L]	Precision [%]	Accuracy [%]	M6 [mg/L]	Precision [%]	Accuracy [%]
1	Chromaticity_R	0.54	8.39	0.63	0.40	6.46	13.63
2	Chromaticity_B	0.51	11.85	6.15	0.37	4.33	5.11
3	V_prom_luv	0.52	12.00	4.31	0.39	7.99	10.79

Regarding Table 13-A, the HR determination yields solid results for M1, particularly with the *V_prom_luv* parameter. M2 presents a concentration higher than the calibration standards. This positioning outside the linear range results in a high number of experimental points falling beyond the interpolation limits, leading to an elevated RSD. Because few valid data points were available, the margin to discard outliers was severely restricted, forces the inclusion of less accurate values that degrade the final metrics.

For Table 13-B, the analytical performance varies significantly between samples. The quantification of M3 shows robust and consistent behaviour across all evaluated colour parameters. The results for **M4** reveal lower performance in either precision or accuracy depending on the coordinate selected, indicating that the determination of this specific sample of this concentration level are

affected by their proximity to the low limit of calibration range. Table X-C outlines that for **M5**, the system demonstrates acceptable robustness, though accompanied by slightly elevated precision errors around 10%. For **M6,** while the precision metrics show a clear improvement, the accuracy error was higher due probably to the same reason discussed for M4.

In conclusion, the use of this cell with multiple optical paths provides adequate results for the quantification of different types of water, although the accumulation of waste poses a significant difficulty for its reuse, especially for the quantification of samples with a low concentration level.

10.2. DESIGN REFINEMENT VIA A METHACRYLATE CELL FOR ENHANCED SAMPLE DETERMINATION

To mitigate the structural imperfections related to surface roughness, chemical staining, and potential fluorescence interference, an identical cell architecture featuring equivalent channels and staircase steps was fabricated using polymethyl methacrylate. The experimental procedure remained identical to the previous section, limiting the evaluation to samples M1 and M2 for the high-range determination, and M3 and M4 for the low-range framework. The resulting image captures for these runs are presented in Figure 21.

Figure 21. Smartphone digital image captures for real sample quantification utilizing the PMMA-based cell: (left) samples M1 and M2 for HR determination and (right) samples M3 and M4 for LR determination.

The calibration metrics for the **commercial high-range determination** is presented in Table X-A, while the experimental quantification results for the corresponding real samples M1 and M2 are summarized in Table 14-B. Figure 22 illustrates the calibration curve for the *Cromaticity_B* (left) and *V_prom_luv* (right) parameter across its linearity interval.

Table 14-A. Validation metrics for MOP digital colorimetric determination using the refined methacrylate cell for HANNA HR method.

Entry	Parameter	Interval	Calibration / RMSE [%]	Precision / RSD [%]
1	Chromaticity_R	5.0 mg/L – 60.0 mg/L	2.73	1.29
2	Chromaticity_B	5.0 mg/L – 75.0 mg/L	2.87	0.40
3	V_prom_luv	5.0 mg/L – 100.0 mg/L	2.22	0.68

Table 14-B. MOP analytical results for real samples using the refined methacrylate cell for HANNA HR method.

Entry	Parameter	M1 [mg/L]	Precision [%]	Accuracy [%]	M2 [mg/L]	Precision [%]	Accuracy [%]
1	Chromaticity_R	23.60	1.35	3.67	74.98	9.50	0.73
2	Chromaticity_B	23.57	1.81	3.78	72.47	4.76	4.05
3	V_prom_luv	24.37	3.37	0.51	75.03	2.36	0.66

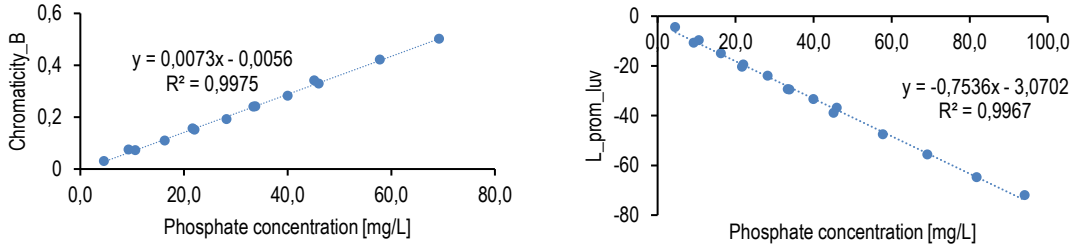

Figure 22. Calibration curve for *Chromaticity_B* (left) and *L_prom_luv* (right) parameter using the refined methacrylate cell for MOP cell for HANNA HR determination of phosphate.

The calibration metrics in Table 14-A and Figure 22 demonstrate that the high-range method behaves as an official analytical standard, exhibiting precision values below 2% and an RMSE under 3%. Furthermore, the linear working ranges were successfully extended for each parameter, reaching up to 60.0 mg/L for *Chromaticity_R*, 75.0 mg/L for *Chromaticity_B*, and 100.0 mg/L for the *V_prom_luv* coordinate, with all profiles displaying an excellent linearity close to unity.

The quantification results for samples M1 and M2 (Table 14-B) demonstrate high accuracy, yielding values that closely converge with those obtained via standard spectrophotometry. Regarding precision, sample M1 exhibits robust metrics across all coordinates with an RSD below 4%. Although sample M2 shows slightly higher deviation values, it represents a substantial improvement by drastically reducing the elevated errors previously obtained with the epoxy resin cell (see Table 13-A).

The calibration metrics for the **commercial low-range determination** is presented in Table 15-A, while the experimental quantification results for the corresponding real samples M3 and M4 are summarized in Table 15-B. Figure 23 illustrates the calibration curve for the *Cromaticity_B* (right) and *V_prom_luv* (right) parameter across its linearity interval.

Table 15-A. Validation metrics for MOP digital colorimetric determination using the refined methacrylate cell for HANNA LR method.

Entry	Parameter	Interval	Calibration / RMSE [%]
1	Chromaticity_R	0.25 mg/L – 3.5 mg/L	2.45
2	Chromaticity_B	0.25 mg/L – 3.5 mg/L	3.69
3	V_prom_luv	0.25 mg/L – 3.5 mg/L	2.75

Table 15-B. MOP analytical results for real samples using the refined methacrylate cell for HANNA LR method.

Entry	Parameter	M3 [mg/L]	Precision [%]	Accuracy [%]	M4 [mg/L]	Precision [%]	Accuracy [%]
1	Chromaticity_R	2.44	5.83	7.41	0.46	6.42	0.55
2	Chromaticity_B	2.47	3.97	6.28	0.45	4.89	3.20
3	V_prom_luv	2.49	8.15	5.78	0.42	3.81	8.11

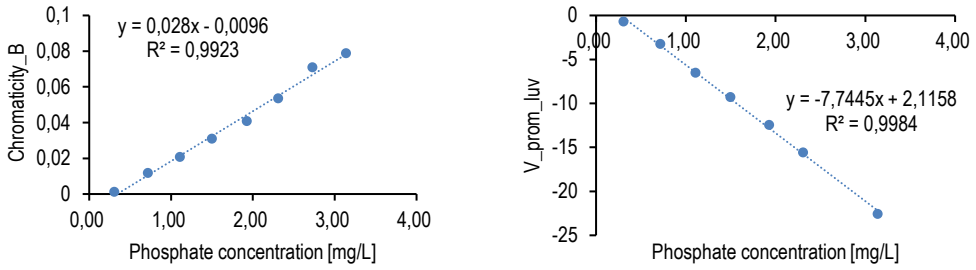

Figure 23. Calibration curve for *Chromaticity_B* (left) and *V_prom_luv* (right) parameter using the refined methacrylate MOP cell for HANNA LR determination of phosphate.

The calibration metrics presented in Table 15-C and Figure 23 confirm the validation of the commercial low-range framework, exhibiting an RMSE below 4% and coefficients of determination close to unity. Notably, the linear dynamic range remains identical to the one established with the epoxy resin cell, spanning consistently from 0.25 to 3.5 mg/L across all parameters. The quantification results for the real water samples (Table 15-B) show that the determination of sample M3 yields similar analytical metrics to those obtained with the epoxy resin cell. Conversely, a substantial improvement is achieved for sample M4, significantly optimizing both its precision and accuracy values.

In conclusion, the PMMA-based cell yields robust results, representing a substantial improvement over the previous epoxy resin prototype in all evaluated analytical scenarios. This optimized design demonstrates that factors such as material fluorescence, surface roughness, and chemical staining explicitly degraded the optical response in earlier configurations. Consequently, by implementing a completely smooth and transparent cell body, these physical interferences were effectively minimized, successfully validating this prototype as the most reliable and efficient architecture for the digital image colorimetry system.

11. SUSTAINABILITY ASSESSMENT FOR METHODOLOGICAL COMPARISON

To objectively evaluate the ten analytical methodologies developed throughout this work, a multi-criteria assessment was performed using the White Analytical Chemistry (WAC) framework. Given that sustainability frameworks lack a universal reference dictionary, these metrics operate as qualitative indices established by consistently applying the same operational criteria across all methods to ensure analytical objectivity. As an example, for the Green Principles (environmental safety), commercial kits received higher ratings than conventional laboratory procedures because they reduce direct handling of hazardous reagents, while smartphone-based systems and the SMOP method achieved the highest scores due to their low reagent consumption, minimal waste generation, and reduced energy requirements. All calculations and scoring criteria used for WAC parameters across all methodologies is provided in Appendix 4. Specifically, Table 4.1 presents the assessment of the Red Principles, Table 4.2 the Green Principles, and Table 4.3 the Blue Principles, while Table 4.4 summarized all data results. Figure 24 presents the comprehensive WAC evaluation of the ten methods developed in this study, displaying a direct and scalable comparison of their analytical performance, environmental impact, and operational efficiency.

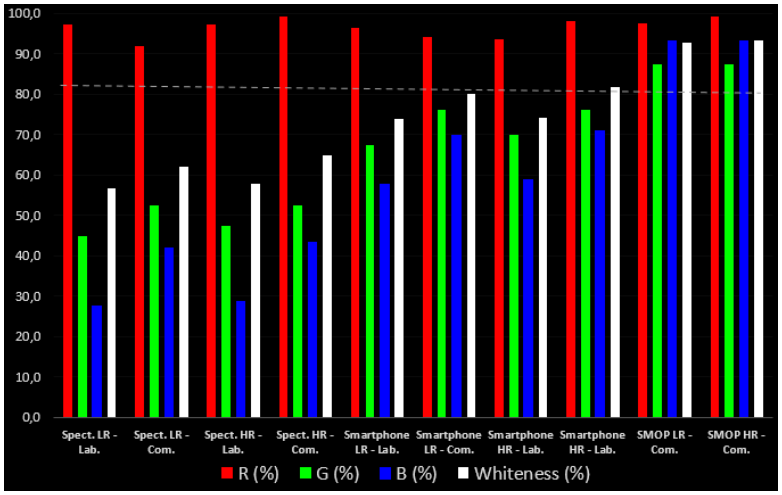

Figure 24. WAC evaluation of the ten analytical methodologies evaluated throughout this work.

As illustrated in Figure 24, the Whiteness Index (WI, %) shows a clear improvement when moving from conventional benchtop methods to decentralised portable platforms. Commercial reagent kits consistently achieve higher scores than laboratory-prepared reagents due to improved safety and reduced chemical handling. Among the evaluated approaches, smartphone-based systems provide the best overall performance, benefiting from their portability, low energy consumption, and reduced waste generation. Figure 25 demonstrates this comprehensive methodological comparison across the entire experimental spectrum, tracing the transition from the most conventional baseline using spectrophotometry with laboratory reagents to the optimised SMOP smartphone platform using commercial kits.

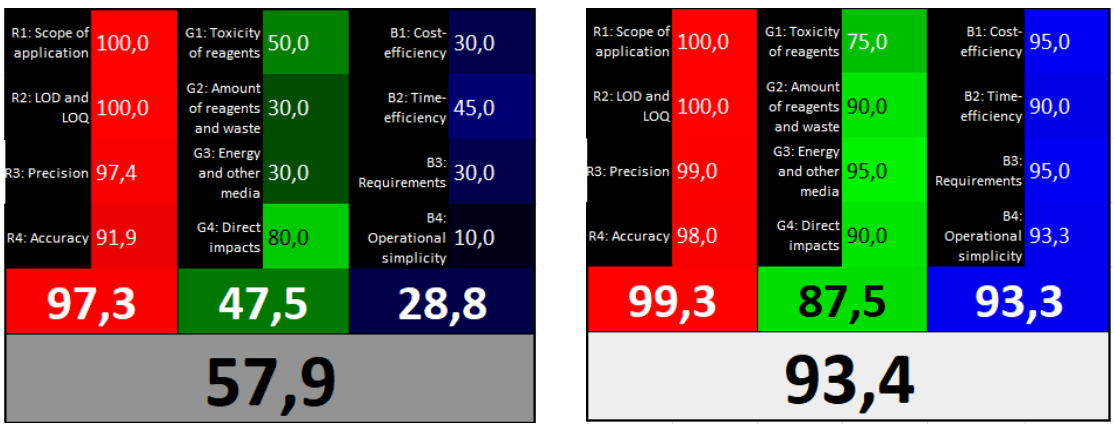

Figure 25. Comparative WAC score matrices for individual operational frameworks: (left) conventional spectrophotometry using laboratory reagents, and (right) smartphone-based SMOP method using commercial reagents.

12. CONCLUSIONS

The conclusions of this bachelor's thesis are systematically presented by analysing, item by item, each of the specific objectives introduced at the beginning of this manuscript.

The evaluation of colorimetric methods using spectrophotometry methods demonstrate that commercial chemical kits yield results that are fully comparable to traditional laboratory reagents. Although conventional laboratory methodologies provide highly robust calibration metrics, the commercial kits offer an optimal balance due to their operational simplicity and practicality during experimental development, thereby technically justifying their selection as the core analytical framework for this resource-efficient analysis.

The evaluation of smartphone colourimetric determinations at a constant volume proved that digital image colorimetry is a viable and robust alternative for water quality analysis. The commercial HANNA methods outperformed the traditional laboratory reagents, demonstrating superior calibration metrics and lower precision errors. Furthermore, the digital calibration curves maintained solid linearity even at the operational range limits, showcasing the high potential of this methodology.

The implementation off smartphone colorimetric determinations at a variable volume demonstrated that varying the sample volume yields quantitative results fully comparable to the classic approach of using different concentrations at a constant volume. Applying a custom illumination mask that is perfectly aligned with the samples significantly enhances the precision metrics of the methodology. Finally, the integration of a background blank correction improves overall analytical performance by successfully providing a robust standardization of the light source.

The analytical behaviour depended on the chemical complex and concentration, showing that the chromaticity parameters R and G stood out as the top candidates for both blue and yellow solutions, while *L_prom_luv* coordinate exhibit an outstanding sensitivity for highly darkened blue solutions. The strategic selection of these diverse parameters successfully expanded the operational linear ranges, thereby offering robust and flexible alternatives during the calibration modelling phase.

The development of the Simultaneous Multi-Optical Path system achieved highly satisfactory results. The methodology establishes a rigorous experimental procedure that is easily implemented, optimizing operational workflow. Furthermore, due to the high density of data points simultaneously generated by the multi-optical path architecture, the system demonstrates an exceptional tolerance to localized experimental errors. This feature allows for the statistical rejection of outlier or aberrant data points without compromising the overall analytical validity, as the remaining dataset ensures enough points to perform robust external calibrations and reliable sample determinations.

Regarding the application to real water samples, the structural transition from a prototype epoxy resin cell to a refined methacrylate architecture fundamentally enhanced the analytical performance of the SMOP system. While the initial epoxy cell yielded limited accuracy and precision metrics due to its material limitations, the optimized methacrylate cell drastically improved the optical clarity and alignment of the measurements. The results obtained with this final device proved that the smartphone-SMOP methodology is fully comparable in terms of analytical reliability, accuracy, and precision to conventional laboratory methods based on reference reagents and classical UV-Vis spectrophotometry. In addition, methacrylate cells can be reused.

Finally, the sustainability and applicability assessment mathematically confirmed the highly resource-efficient nature of the proposed framework. By simultaneously evaluating the economic, analytical, and environmental factors of all the implemented methodologies, the results demonstrated that the Simultaneous Multi-Optical Path system achieves the highest indices of performance and viability. This comprehensive evaluation proves that, in addition to delivering excellent analytical results, this novel method represents a significantly superior alternative in terms of White Analytical Chemistry compared to conventional spectrophotometric and standard digital colorimetry approaches.

The successful fulfillment of these specific objectives has led to the development of a highly resource-efficient and environmentally applicable methodology for the determination of water quality parameters using smartphone-based technology.

13. REFERENCES AND NOTES

1. Shiklomanov, I. A. World Fresh Water Resources. In Water in Crisis: A Guide to the World's Fresh Water Resources; Gleick, P. H., Ed.; Oxford University Press: New York, **1993**; pp 13–24.
2. *RD 817/2015 España. Boletín Oficial del Estado* [Online] **2015**, 219, 80581–80629. https://www.boe.es/eli/es/rd/2015/09/11/817 (accessed June 9, 2026).
3. *RD 35/2023 España. Boletín Oficial del Estado* [Online] **2023**, 21, 10424–10452. https://www.boe.es/eli/es/rd/2023/01/24/35 (accessed June 9, 2026).
4. *RD 509/1996 España. Boletín Oficial del Estado* [Online] 1996, 77, 12019–12023. https://www.boe.es/eli/es/rd/1996/03/15/509 (accessed June 9, 2026).
5. RD 1085/2024 *España. Boletín Oficial del Estado* [Online] **2024**, 256, 133580–133618. https://www.boe.es/eli/es/rd/2024/10/22/1085 (accessed June 9, 2026).
6. RD 3/2023 *España. Boletín Oficial del Estado* [Online] **2023**, 9, 3218–3273. https://www.boe.es/eli/es/rd/2023/01/10/3 (accessed June 10, 2026).
7. Filippelli, G. M. The Global Phosphorus Cycle: Past, Present, and Future. Elements **2008**, 4, 89–95.
8. Smith, V. H.; Schindler, D. W. Eutrophication of Freshwater and Marine Ecosystems. Limnol. Oceanogr. **2009**, 54, 2284–2296.
9. Richardson, K.; Steffen, W. et. all Earth Beyond Six of Nine Planetary Boundaries. Science **2023**, 381, adh2458.
10. U.S. Geological Survey. Phosphate Rock. In Mineral Commodity Summaries; U.S. Department of the Interior: Reston, VA, **2024**; pp 130–131.
11. Yuan, Z.; Pratt, S.; Batstone, D. J. Phosphorus Recovery from Wastewater through Microbial Processes. Water Res. **2012**, 46, 5183–5197.
12. Egle, L.; Rechberger, H.; Zessner, M. Overview and Description of Technologies for Phosphorus Recovery from Sewage Sludge and New Disease Regulations. Resour., Conserv. Recycl. **2015**, 105, 325–346.
13. European Commission. Study on the Critical Raw Materials for the EU 2023: Final Report; Publications Office of the European Union: Luxembourg, **2023**; pp 45–52.
14. Guidry, M. W.; Mackenzie, F. T. Apatite Dissolution Kinetics and the Long-Term Phosphorus Cycle. Chem. Geol. **2003**, 202, 85–101.
15. Rice, E. W.; Baird, R. B.; Eaton, A. D., Eds. 4500-P Phosphorus. In Standard Methods for the Examination of Water and Wastewater, 23rd ed.; American Public Health Association, American Water Works Association, Water Environment Federation: Washington, DC, **2017**; pp 4-146–4-155.
16. Hanna Instruments. Water Analysis Handbook, 4th ed.; Woonsocket, RI, **2019**; Method HI93706 Phosphorus, Low Range, pp 412–415.
17. Hanna Instruments. Water Analysis Handbook, 4th ed.; Woonsocket, RI, **2019**; Method HI93738 Phosphorus, High Range, pp 416–420.
18. Capitán-Vallvey, L. F.; López-Ruiz, N.; Martínez-Olmos, A.; Erenas, M. M.; Palma, A. J. Recent Developments in Chemical Sensing Platforms Based on Smartphones. Anal. Bioanal. Chem. **2015**, 407, 6177–6192.
19. Schanda, J. Colorimetry: Understanding the CIE System; Wiley-Interscience: Hoboken, NJ, **2007**; pp 61–83.
20. Xing, Y.; Xue, B.; Lin, Y.; Wu, X.; Fang, F.; Qi, P.; Guo, J.; Zhou, X. A Cellphone-Based Colorimetric Multi-Channel Sensor for Water Environmental Monitoring. Front. Environ. Sci. Eng. **2022**, 16 (12), 155. https://doi.org/10.1007/s11783-022-1590-z.
21. Ai, H.; Zhang, K.; Zhang, H. Efficient Smartphone-Based Measurement of Phosphorus in Water. Water Res. X 2024, 22, 100217. https://doi.org/10.1016/j.wroa.**2024**.100217.
22. Pena-Pereira, F.; Wojnowski, W.; Tobiszewski, M. AGREE—Analytical Greenness Metric Approach and Software. Anal. Chem. **2020**, 92, 10076–10082.

All information, experimental materials, and data derived from this work are compiled in a OneDrive folder, the access link to which is provided below.

Rodríguez, Mateo. *Comprehensive Repository of Experimental Data and Materials for Water Quality Monitoring* [OneDrive Cloud Repository]. TFG_2025_2026_Mateo_Aguas_Smartphone_2 (accessed June 10, 2026); access available upon invitation/request.

Additionally, the spreadsheet containing all raw data and calculations for the WAC assessment (see Section 11) is provided bellow.

Rodríguez, Mateo. *White Analytical Chemistry Index Calculator for Phosphate Determination Methods* [Excel Spreadsheet]. WAC evaluation.xlsx (accessed June 10, 2026). access available upon invitation/request.

14. ACRONYMS

ACS: American Chemical Society

AGREE: Analytical Greenness Metric Approach

ATP: Adenosine Triphosphate

CIE: Commission Internationale de l'Éclairage

CC BY: Creative Commons Attribution

CMOS: Complementary Metal–Oxide–Semiconductor

CVOP: Continuously Variable Optical Pathlength

DIC: Digital Image Colorimetry

DNA: Deoxyribonucleic Acid

EBPR: Enhanced Biological Phosphorus Removal

EU: European Union

GAC: Green Analytical Chemistry

HR: High Range

HTML: HyperText Markup Language

ICP-AES: Inductively Coupled Plasma Atomic Emission Spectroscopy

ICP-MS: Inductively Coupled Plasma Mass Spectrometry

IFAS: Integrated Fixed-film Activated Sludge

ISO: International Organization for Standardization

LR: Low Range

MBR: Membrane Bioreactor

NIST: National Institute of Standards and Technology

NYL: Nylon

PA: Pro Analysi

PMMA: Polymethyl Methacrylate

RD: Real Decreto

RE: Relative Error

RGB: Red, Green, Blue

RMSE: Root Mean Square Error

RNA: Ribonucleic Acid

RSD: Relative Standard Deviation

SMOP: Simultaneous Multi-Optical Path

TP: Total Phosphorus

UV-Vis: Ultraviolet-Visible

WAC: White Analytical Chemistry

WI: Whiteness Index

WWTP: Wastewater Treatment Plant

XLSX: Microsoft Excel Open XML Spreadsheet

APPENDICES

APPENDIX 1: SUPPLEMENTARY CALIBRATION DATA FOR LABORATORY REAGENTS UNDER VARIABLE VOLUMES

The supplementary data presented in this appendix corresponds to Section 8.1.

Table 1.1. Validation metrics for digital colorimetry determination evaluating variable volumes for molybdate-vanadate method.

Entry	Parameter	Interval	Calibration / RMSE [%]	Precision / RSD [%]	Accuracy / RE [%]
1	Chromaticity_R	7.0 mg/L – 50.0 mg/L	3.08	0.45	6.07
2	Chromaticity_B	7.0 mg/L – 50.0 mg/L	3.64	1.54	3.99
3	V_prom_luv	7.0 mg/L – 50.0 mg/L	5.60	2.72	4.29

Table 1.2. Validation metrics for digital colorimetry determination evaluating variable volumes for molybdenum blue method.

Entry	Parameter	Interval	Calibration / RMSE [%]	Precision / RSD [%]	Accuracy / RE [%]
1	Chromaticity_R	0.40 mg/L – 3.00 mg/L	9.41	0.85	6.85
2	Chromaticity_B	0.40 mg/L – 3.00 mg/L	10.40	0.29	5.56
3	V_prom_luv	0.40 mg/L – 3.00 mg/L	9.52	10.76	6.87

APPENDIX 2: SUPPLEMENTARY CALIBRATION DATA FOR LABORATORY REAGENTS UNDER VARIABLE VOLUMES AND ILLUMINATION MASK IMPLEMENTATION

The supplementary data presented in this appendix corresponds to Section 8.2.

Table 2.2. Validation metrics for digital colorimetry at variable volumes using the illumination mask for molybdate-vanadate method.

Entry	Parameter	Interval	Calibration / RMSE [%]	Precision / RSD [%]	Accuracy / RE [%]
1	Chromaticity_R	5.0 mg/L – 50.0 mg/L	5.88	1.58	2.38
2	Chromaticity_B	5.0 mg/L – 50.0 mg/L	4.10	0.08	4.75
3	V_prom_luv	5.0 mg/L – 50.0 mg/L	4.35	0.21	3.32

Table 2.2. Validation metrics for digital colorimetry at variable volumes using the illumination mask for molybdenum blue method.

Entry	Parameter	Interval	Calibration / RMSE [%]	Precision / RSD [%]	Accuracy / RE [%]
1	Chromaticity_R	0.40 mg/L – 3.00 mg/L	9.93	0.27	7.91
2	Chromaticity_B	0.40 mg/L – 3.00 mg/L	7.21	0.08	11.61
3	V_prom_luv	0.40 mg/L – 3.00 mg/L	8.47	2.04	7.91

APPENDIX 3: SUPPLEMENTARY CALIBRATION DATA FOR BACKGROUND BLANK CORRECTION

The supplementary data presented in this appendix corresponds to Section 8.3.

Table 3.1. Comparison of validation metrics for molybdate-vanadate method before and after applying the background blank correction.

Entry	Parameter	Backgroung correction	Calibration / RMSE [%]	Precision / RSD [%]	Accuracy [%]
1	Chromaticity_R	No	3.08	0.45	6.07
2	Chromaticity_R	Yes	3.33	0.39	2.48
3	Chromaticity_B	No	3.64	1.54	3.99
4	Chromaticity_B	Yes	3.73	1.82	1.48
5	V_prom_luv	No	5.60	2.72	4.29
6	V_prom_luv	Yes	6.45	3.00	1.37

Table 3.2. Comparison of validation metrics for molybdenum blue method before and after applying the background blank correction.

Entry	Parameter	Background correction	Calibration / RMSE [%]	Precision / RSD [%]	Accuracy [%]
1	Chromaticity_R	No	9.41	0.85	6.85
2	Chromaticity_R	Yes	7.03	0.64	4.37
3	Chromaticity_B	No	10.40	0.29	5.56
4	Chromaticity_B	Yes	3.61	0.33	8.38
5	V_prom_luv	No	9.52	10.76	6.87
6	V_prom_luv	Yes	7.58	2.59	7.65

Table 3.3. Comparison of validation metrics for HANNA LR method before and after applying the background blank correction.

Entry	Parameter	Background correction	Calibration / RMSE [%]	Precision / RSD [%]	Accuracy [%]
1	Chromaticity_R	No	3.81	1.45	2.91
2	Chromaticity_R	Yes	3.71	0.52	2.22
3	Chromaticity_B	No	4.42	1.09	3.20
4	Chromaticity_B	Yes	3.02	0.36	4.79
5	V_prom_luv	No	5.36	8.38	5.37
6	V_prom_luv	Yes	4.69	1.86	4.39

APPENDIX 4: SUPPLEMENTARY DATA AND CALCULATIONS FOR WHITE ANALYTICAL CHEMISTRY (WAC) ASSESSMENT

The supplementary data presented in this appendix corresponds to Section 11.

Table 4.1. Scoring matrix of the Red Principles for the analytical performance across all the evaluated methods.

			R1: Scope of application	R2: LOD and LOQ			R3: Precision			R4: Accuracy			
RED PRINCIPLES (analytical performance)	Method number	Method name	0-100	LOD	LOQ	0-100	RSD% (repeatability)	RSD% (reproducibility)	0-100	Relative error (%)	Recovery (%)	0-100
	1	Spect. LR - Lab.	100	0,02	0,05	100	2,74	2,74	94,5	4,89		95,1
	2	Spect. LR - Com.	100	0,02	0,05	100	1,32	1,32	90,8	8,08		77,5
	3	Spect. HR - Lab.	100	1	3	100	4,58	4,58	97,4	22,55		91,9
	4	Spect. HR - Com.	100	1	3	100	1,26	1,26	97,5	0,8		99,2
	5	Smartphone LR - Lab.	100			100			95			91
	6	Smartphone LR - Com.	100			100			89			88
	7	Smartphone HR - Lab.	100			100			93			81
	8	Smartphone HR - Lab.	100			100			98			94
	9	SMOP LR - Com.	100			100			95			95
	10	SMOP HR - Com.	100			100			99			98

Table 4.2. Scoring matrix of the Green Principles for the environmental sustainability across all the evaluated methods.

			G1: Toxicity of reagents (impact and biodegradation)		G2: Amount of reagents and waste			G3: Concumption of energy and other media	G4: Direct impacts (safety, use of animals and GMOs)			
GREEN PRINCIPLES (green chemistry)	Method number	Method name	Total number of pictograms	0-100	Reagent consumption	Waste production	0-100	1-100	Occupational hazards	Safety of users (0-100)	Use of animals (0 if no, 1 if yes)	Use of GMO (0 if no, 1 if yes)
	1	Spect. LR - Lab.		40			30	30		40	0	0
	2	Spect. LR - Com.		60			30	30		70	0	0
	3	Spect. HR - Lab.		50			30	30		40	0	0
	4	Spect. HR - Com.		60			30	30		70	0	0
	5	Smartphone LR - Lab.		40			55	95		40	0	0
	6	Smartphone LR - Com.		60			60	95		70	0	0
	7	Smartphone HR - Lab.		50			55	95		40	0	0
	8	Smartphone HR - Lab.		60			60	95		70	0	0
	9	SMOP LR - Com.		75			90	95		70	0	0
	10	SMOP HR - Com.		75			90	95		70	0	0

Table 4.3. Scoring matrix of the Blue Principles for the finnancial viability across all the evaluated methods.

			B1: Cost-efficiency		B2: Time-efficiency		B3: Requirements			B4: Operational simplicity		
BLUE PRINCIPLES (practical side)	Method number	Method name	Total cost	0-100	Speed of analysis	0-100	Sample consumption	Sample consumption (0-100)	Other needs: advanced instruments, skills, facilities (0-100)	Miniaturization (0-100)	Integration and automation (0-100)	Portability (0-100)
	1	Spect. LR - Lab.		30		40		50	10	0	30	0
	2	Spect. LR - Com.		40		75		50	30	0	40	0
	3	Spect. HR - Lab.		30		45		50	10	0	30	0
	4	Spect. HR - Com.		40		80		50	30	0	40	0
	5	Smartphone LR - Lab.		70		45		65	50	50	50	75
	6	Smartphone LR - Com.		75		75		65	70	50	60	75
	7	Smartphone HR - Lab.		70		50		65	50	50	50	75
	8	Smartphone HR - Lab.		75		80		65	70	50	60	75
	9	SMOP LR - Com.		95		90		95	95	95	85	100
	10	SMOP HR - Com.		95		90		95	95	95	85	100

Table 4.4. Percentage values obtained for the Red, Green, Blue, and global Whiteness indices for each of the evaluated analytical methods.

Method number	Method name	R (%)	G (%)	B (%)	Whiteness (%)
1	Spect. LR - Lab.	97,4	45,0	27,5	56,6
2	Spect. LR - Com.	92,1	52,5	42,1	62,2
3	Spect. HR - Lab.	97,3	47,5	28,8	57,9
4	Spect. HR - Com.	99,2	52,5	43,3	65,0
5	Smartphone LR - Lab.	96,5	67,5	57,7	73,9
6	Smartphone LR - Com.	94,3	76,3	69,8	80,1
7	Smartphone HR - Lab.	93,5	70,0	59,0	74,2
8	Smartphone HR - Lab.	98,0	76,3	71,0	81,8
9	SMOP LR - Com.	97,5	87,5	93,3	92,8
10	SMOP HR - Com.	99,3	87,5	93,3	93,4